South African Journal of Chemical Engineering 40 (2022) 209–229

Contents lists available at ScienceDirect

South African Journal of Chemical Engineering

journal homepage: www.elsevier.com/locate/sajce

Adsorption of lead (Pb-II) using CaO-NPs synthesized by solgel process from hen eggshell: Response surface methodology for modeling, optimization and kinetic studies

Ramachandran Kasirajan *, Abreham Bekele, Ermias Girma

School of Chemical Engineering, Jimma Insitute of Technology, Jimma University, Jimma, Ethiopia

ARTICLE INFO

Keywords:
Calcium oxide nanoparticles
Lead removal
Adsorption isotherms and kinetics
Hen eggshell
Solgel process
Optimization by response surface methodology

ABSTRACT

In this research study, the application of synthesized calcium oxide nanoparticles by sol-gel process from a waste resource of hen eggshells for the adsorption of lead ion from aqueous solutions was investigated. Characteristic behavior of the CaO-NPs like porosity, point of zero charges, Fourier transform infrared radiation spectroscopy, X-ray diffraction, specific surface area, thermal gravimetric analysis, and scanning electron microscopy was analyzed. X-ray diffraction discovered that the size of synthesized calcium oxide nanoparticles was 24.34 nm and the specific surface area was 77.4m^2/g by Sears method. The removal of divalent lead from aqueous solutions was optimized by using response surface methodology. The optimum percentage of lead removal (99.07%) resulted at initial concentration 75.46 ppm, pH 6.94, adsorbent dosage 0.838 g, and contact time 101.97 min. The experimental removal efficiency (98.86%) agreed very well with the predicted one (99.07%), showing the suitability of the model used and the success of response surface methodology in optimizing of removal of Pb (II) ions from aqueous solutions. The lead removal was well fitted into the Langmuir isotherm model with correlation coefficients of 0.9963. The adsorption kinetic data effectively fitted to the pseudo-first-order model with good correlation coefficients of 0.945. The pseudo-second-order model was the rate-limiting step in the lead (II) adsorption process with CaO NPs. From he above output we have conclude that, the calcium oxide nanoparticles prepared from eggshell have a good capacity for the removal of the lead from the aqueous solutions.

1. INTRODUCTION

The contamination of water resources by industrial effluents holding toxic heavy metals is an issue of great concern for the reason that their non-biodegradable and polluting environment (Afroze and Sen, 2018). Heavy metals are largely engaged in the textile industry, acid battery manufacturing, agricultural, household wastewater, metallurgical operation, glass industry, and ceramics are the main sources of heavy metal contaminations in the wastewater. Lead is one of the severe metals between toxic heavy metals (Fatemeh Safatian, 2019). Very low concentrations of lead-heavy metals in drinking water cause diseases like encephalopathy, hepatitis, kidney damage, blood pressure, abortion, improper function in the brain, and the central nervous system of unborn children when it enters a fetus through the placenta of the mother (Volesky, 1990). Environmental legislation obliges industries to eliminate heavy metals from their toxic-containing effluents before disposal into the water. Because of the low-income limit, a lot of industries are not successful to provide investment costs in pollution remediation apparatus and technologies (EEPA, 1997). The owners of industries that have enough capital have no interest to fit efficient treatment technologies, because of weak governmental control and weak environmental policy implementation. Environments can be affected by heavy metal pollution. It stays for a long period of time in soil and aqueous solution and can not be decomposed like other organic pollutants. Pollutant heavy metals are all soluble at low PH, and consequently, toxicity problems are relatively higher in the environments. Several treatment methods have been adopted to remove heavy metals from wastewater, which can be divided into physical, chemical, and biological methods. In comparison to the other physical, chemical, and biological methods available for the treatment of wastewater industry effluents, adsorption is the most preferred technique due to its simple, flexible design and easy operation. Common adsorbents like activated carbon, silica gel, activated alumina, and ion exchange resins have a good capacity for removing pollutants, but their main disadvantages refer to their high

* Corresponding author.
E-mail address: ramachandran.kasirajan@ju.edu.et (R. Kasirajan).

https://doi.org/10.1016/j.sajce.2022.03.008
Received 30 March 2021; Received in revised form 25 February 2022; Accepted 22 March 2022
Available online 24 March 2022

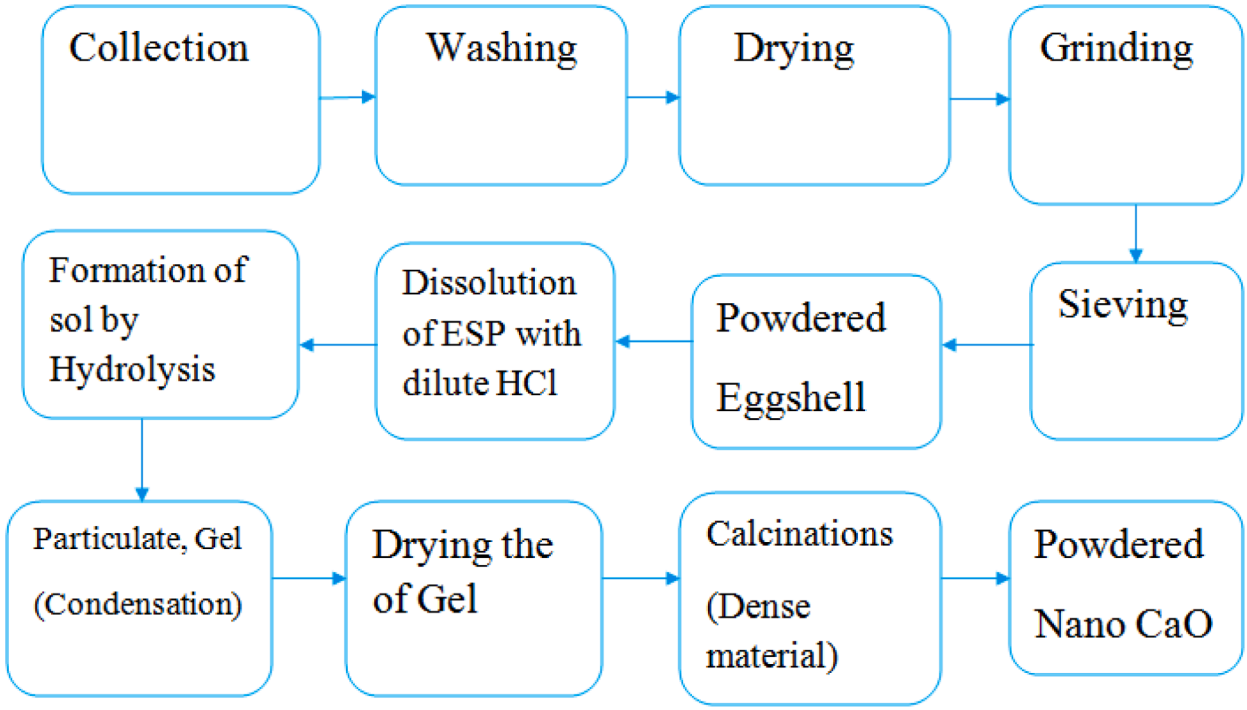

Fig. 1. Process flow for preparation of CaO adsorbent from waste hen eggshells.

installation and operating cost of treatment and difficult regeneration, which increases the wastewater treatment cost (Stadelman, 2000). Different forms of biomass can be used for the removal of lead pollutants from the point and non-point sources of effluents. However, only a piece of research was done on the sorption studies using eggshell-based CaO particles as bio adsorbents. Interaction effects that occur among process variables were not included (Achla Kaushal, 2017). The other gap could be few researchers use raw hen eggshell as an adsorbent for heavy metal removal from wastewater but it had small removal efficiency because it lacks porosity and lacks large surface areas. Therefore synthesizing calcium oxide nanoparticles from hen eggshells overcomes the problems. Waste hen eggshells represent traditionally useless substances from the processors and cause unpleasant odors from biodegradation, damaging microbial activity, altering characteristics of the soil (Castro, 2011). The effective uses of waste chicken eggshells are to substitute the commercial of calcium carbonate, calcium hydroxide, and calcium oxide to eliminate the waste problem in the household, conservation of natural resources like rock and soil to reduce the global greenhouse effect.

Due to the low-cost and large availability, waste hen eggshells become used as an adsorption process, an attractive and promising technology. Hen eggshell, the main component of pure calcium carbonate (Adeyeye, 2009), is important in the heavy metal removal from wastewater but has less removal efficiency because of its little porosity. Therefore, synthesizing calcium oxide particles from hen eggshells by sol-gel derived overcomes the shortcomings of the bulk material users because of better performance in terms of higher surface area to its volume ratio, it imparts size-dependent properties such as higher adsorption tendency and large volume rapid wastewater treatment systems. Communities around low land; low-lying areas severe in drinking water, livestock, irrigation for agriculture, and amusement due to their dependency on rivers and lakes. In Addis Ababa, the capital city of Ethiopia, total wastewater discharged annually is 49 million m^3 in volume, from this 4 million m^3 is industrial effluents, only 4% of industrial effluents are being treated and reused. Heavy metals that are released from industries are lead, cadmium, cobalt, mercury, zinc, iron, nickel, and copper which are poisonous to humans, animals, and aquatic life. Among all, lead Pb (II) is dangerous and has the potential for cancer. Because of its abundance in industries as point sources and agriculture as non-point sources, it will become above the allowable limit which is put by Environmental Protection agencies of Ethiopia (Fenta, 2014). Ethiopia has no capacity to use advanced wastewater treatment technologies to overcome industrial effluents, consequently, it is important to use locally available hen eggshells agricultural biowaste, sources of calcium oxide nanoparticles for the removal of lead ions from aqueous solutions. Waste hen eggshells that are disposed of as garbage have zero economic value. The best alternative way to convert waste hen eggshells to high economic value products can be to alter them into calcium oxide nanoparticles as an adsorbent of industrial heavy metals. It is a promising contribution to treating contaminated wastewater before being released into the water bodies and environments. The uses of other agricultural precursors like sawdust (Fathia, 2017), tea waste (Geeta, 2014), and sesame husks (Zhang, 2012) for the preparation of activated carbon have been studied in detail by different researchers. However, no adequate research to investigate these issues, particularly in high-purity calcium oxide nanoparticles based on Ethiopian chicken eggshell, with low cost, additives, expensive equipment, and no pressure to produce adsorbents to remove heavy lead metals from wastewater. Therefore, this study aims to treat lead contamination before it is released into water bodies or the environment using locally available chicken eggshells that contain the nanoparticles CaO as an adsorbent. . This study intended to remove lead (II) from an aqueous solution using calcium oxide nanoparticles as a potential low-cost adsorbent. The effect of operating parameters like pH, contact time, adsorbent dosage, and initial metal concentration was studied in a batch adsorption experiment. Adsorption isotherms and kinetics models were carried out during this study.

The main objective of this research was to study the application of eggshell-derived CaO nanoparticles as an noval adsorbent was synthesized by sol-gel process for the removal of ions from synthetic wastewater. Specific Objectives: To study the proximate analysis of hen eggshells; To prepare CaO adsorbent from eggshells and characterize the adsorbent nanoparticles; To examine the effect of the initial concentration of the adsorbates, pH, contact time, and adsorbent dosage by using batch adsorption technique; and To analysis the adsorptive

capacity and equilibrium isotherm of CaO nanoparticle under batch adsorptive experiment.

2. MATERIALS AND METHODS

2.1. Materials

The chemicals used for the study were analytical grade Pb (II)NO_3 for standard metal ion sample preparation, sodium hydroxide (NaOH) - purity 99.9%, and hydrochloric acid (HCl) – purity 35% were used to adjust the pH value of the solution during the adsorption experiment and shorten the gelation time during CaO nanoparticle synthesis. 1, 5 diphylthiocarbazone (dithizone) – purity 98%: This was a photometric reagent that was used to generate colored water-insoluble complexes with a large number of metal ions. H_2SO_4 (98% purity): was used to bring the apparent pH of the acetone and lead nitrate solution to 5.5. Acetone (99.5% purity): was a solvent used to dissolve an aqueous salt suspension for spectrophotometric measurements. Sodium chloride (NaCl) – purity 99%: was used as an electrolyte during the determination of the point of charge of the adsorbent surfaces. Distilled water was used for different experiments in this research. Nitrogen gas was used as an inert atmosphere to avoid oxidation with the sample during thermal treatment.

2.2. Methods

2.2.1. Sample preparation and pretreatment

Since hen eggshell was the selected adsorbent for the preparation of CaO nanoparticles. Waste hen eggshells were collected from the local areas, from restaurants, bakery houses, and chicken poultry places in Jimma city, Ethiopia. After collection, the waste hen eggshells were first washed completely with tap water to remove dust, impurities, and organic matters adhered on the surface of the eggshells, followed by another cleaned with distilled water several times. Then the efficiently washed eggshells were oven-dried at 150°C for 3hr to remove water (Kumaraswamy, 2015). The dried eggshells were ground by a grinder machine to get the fine powder. The fine eggshell powder was passed through a sieve mesh of 100μm to obtain the finest eggshell powder. The obtained eggshell powder then was kept in a soft polythene bag and placed in a sealed plastic container.

2.2.2. Preparation of Calcium Oxide Nanoparticles

Calcium oxide nanoparticles were synthesized (Figure 1 and Supplimentary file figure S1) from powdered hen eggshells by sol-gel derived technique. Sol-gel was a wet chemical process that comprises the formation of an inorganic colloidal suspension in a continuous liquid to form a three-dimensional network structure. Calcium oxide nanoparticles synthesis by sol-gel were obtained at ambient temperature contributing to less energy consumption, with low cost, no additives, a shorter time during preparation, and no pressure. Due to this, it is cheap, green, and sustainable (Lulit et al ., 2019).

Hen eggshell based calcium oxide nanoparticles synthesis with constant reaction parameters were conducted as the following procedures:

- Ø Preparation of metallic salt, $CaCl_2$ by dissolving powdered raw eggshell in (36%) dilute hydrochloric acid. 0.013gm raw eggshell powder (RESP) was dissolved in 0.25L of 1M hydrochloric acid (HCl).

$$ESP/CaCO_3\ (s) + 2HCl\ (aq) \rightarrow CaCl_2\ (aq) + H_2O\ (l) + CO_2\ (g) \quad (2.1)$$

- Ø Generation of sol by hydrolysis reaction. In an aqueous solution, the hydrolysis reaction brings the system more alkaline. Due to this, it had a high ion-exchange capacity.Sol is a colloidal solution made of solid particles a few hundred nm in diameter, suspended in a liquid phase. By hydrolysis reaction process metal hydroxide was formed. 1M in 250ml, caustic soda (98.5%) concentration was added drop by drop to change the solution sodium chloride generated in equation (3.1) above into sol at room temperature. The gradual addition of aqueous caustic soda to the solution was to give precipitation of calcium hydroxide one over another generating a highly crystalline gel.

$$CaCl\ (aq) + 2Na\ (OH)_2\ (aq) \rightarrow Ca\ (OH)_2\ (s) + 2NaCl\ (aq) \quad (2.2)$$

- Ø The gel was generated by a condensation reaction. A condensation reaction occurred when two molecules join to form a larger molecule and release a smaller molecule (s) in the process. Here the smaller molecule lost in the reaction was the solution sodium chloride. Calcium hydroxide, gel containing solution stayed for 48 hrs at ambient temperature to condense very well. Filtration was the next activity after condensation with the help of a centrifuge at 3000rpm to obtain Ca $(OH)_2$ gel. The filtered Ca $(OH)_2$ was washed with distilled water to get rid of impurities from the precipitate (N. A. Oladoja et al., 2011).
- Ø Then finally water was removed from the generated gel by drying at 60 °C for 24 hr in the oven. And lastly, calcine the dried powder at 900°C for 1 hr using a muffle furnace.

$$Ca\ (OH)_2\ (s) + Hea \rightarrow CaO\ (s) + H_2O\ (l) \quad (2.3)$$

2.2.3. Characterization of eggshell bio sorbent

Proximate analysis: For the hen eggshell /CaO sample as an adsorbent, the physicochemical characteristics like The moisture content of determined by the oven drying method. This was carried out at a temperature of 105°C in accordance with the ASTM D2867-91, Ash content was defined as the quantity of mineral matter which remains as incombustible of testing substance. Ash content determination was done according to the ASTM D2866-94 standard method, The volatile matter was determined according to ISO 562/197. The fixed carbon of the sample was calculated by subtracting the addition of moisture content, ash content (%), and volatile matter (%). The density of the particle (ρ_p) of both powdered raw eggshell and synthesized CaO particle were calculated using the standard vessel for determining relative density (pycnometer). The bulk density (ρ_B) was evaluated based on ASTM D2854-96 standard method. The Hen eggshell powder/CaO particle porosity was evaluated by equation 2.4 (Ketsela et al., 2020).

$$\text{Porosity}\ (\varepsilon_B) = \frac{Particle\ density - Bulk\ density}{Particle\ density} \quad (2.4)$$

Fourier-transform infrared spectroscopy (FT-IR): The FTIR investigation was conducted on bio sorbent of raw eggshells, and CaO to determine the various organic and inorganic groups (functional group) on the surface of adsorbent using spectrum 65 FT-IR (Perkinelmer) model in a range of 4000-400 cm^{-1} using single-crystal potassium bromide mode. First, the RESP/CaO nanoparticles were mixed with the potassium bromide to make it suitable for infrared analysis (Workeneh et al., 2019). Then the mixture was pressed to a small thickness metal less than 1mm, needed for FITR spectroscopy analysis. The wavenumbers associated with signals in the FTIR spectra from chemical functional groups were determined.

X-ray diffraction (XRD) Analysis: X-ray diffraction (XRD) analysis was carried out to know the mean size of single-crystal CaO nanoparticles. It was performed by XRD analytical apparatus equipped with a mono achromatized function at 40KV and a current of 15mA with Cuαradiation (λ=0.154060nm). The sample was analyzed using a double crystal wide angle geometry with the 2θ scan from10-90°. The study of matter at the atomic level was a difficult task but the discovery of electromagnetic radiation with 1 Å (10^{-10}m) wavelength, appearing in

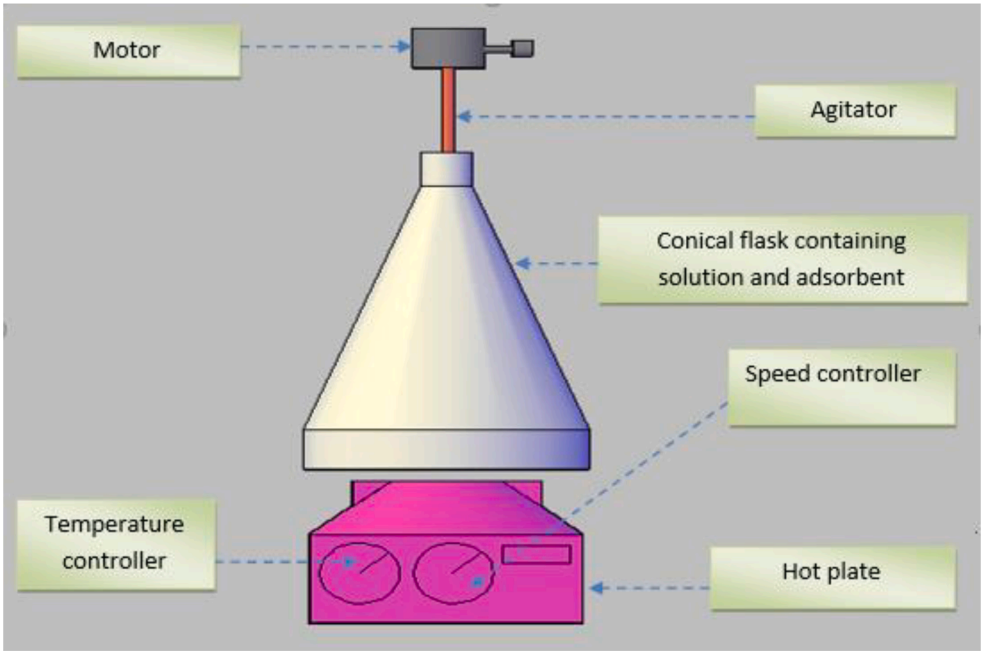

Fig. 2. Experimental Set Up of Batch Adsorption.

the region between gamma-rays and ultraviolet, makes it possible. As the atomic distance in the matter is comparable with the wavelength of X-ray, diffraction finds its nature and gives many significant results related to the crystalline structure. The XRD is used to determine the structure, how the atoms pack together in the crystalline state, what the angle and interatomic distance are etc. Therefore, X-ray diffraction has become a very important and powerful tool for structural characterization in solid-state substances. The crystal size calculation was performed using Scherer's formula (Balaganesh et al., 2018).

Thermal gravimetric analysis (TGA): Thermogravimetric analysis (TGA) is one of the most widely used thermal methods. It is based on the measurement of weight (mass) loss of solid substances as a function of temperature. This is used to analyze the decomposition temperature of raw eggshell powder, calcium hydroxide, and CaO particles with platinum crucible at a heating rate of 10°C/min from ambient temperature to 1000°C. Thermal properties of them were observed by using TGA. The thermogravimetric analyzer was analyzed with the function of temperature. The weight loss of the material was determined from the TGA curve (Li et al., 2020).

Emission Scanning Electron microscope (SEM): the size, shape, and surface morphology of the particles were examined through SEM at an accelerating voltage of 15kV. The scanning electron microscope helps a focused beam of high-energy electrons to produce different types of signals at the surface of solid specimens. The signal produces from electron gives the information about the sample including external morphology, crystalline structure, orientations of materials, and chemical composition of the sample. Using SEM techniques, areas ranging from approximately 1 cm to 10 microns in width can be imaged in the scanning mode with magnification ranging from 20X to 30, 000X, and spatial resolution of 50 to 100 nm. The SEM has the ability for performing analysis of selected point locations of the sample; this approach is especially useful qualitatively for determining chemical compositions, crystal orientations, and crystalline structure (Ramachandran et al., 2011).

Point of Zero Charge (Pzc): The Pzc is the surface chemistry relating to the process of adsorption and it decides the way being when the electrical charge density on the surface is zero. In this research study, nine 250ml of 0.1M NaCl solution conical flask were prepared and their initial pH (pHi) values were adjusted to 2, 3, 4, 5, 6, 7, 8, 9 and10 by dropwise use of 0.1M of either NaOH or HCl for solution needed using a pH meter. The total volume of the mixture of the solution in each flask was made precisely to 50ml by adding 0.1 M NaCl solution of the same strength. 0.5g of CaO nanoparticles used as an adsorbent was added into each solution holding conical flasks which were capped immediately. The mixture of the solution was made to equilibrate at 200rpm in incubating shaker at room temperature for 24hr until pH of the solution doesn't change (Workeneh et al., 2019). The solution was then filtered with a vacuum filter and the final filtrates pH (pHf) values were measured and noted. Then the difference between the final and initial pH (ΔpH) values in the y-axis was plotted against the x-axis (pHi). The point of intersection of the outcoming curve with the x-axis gave the pHpzc.

Specific Surface Area: The specific surface area of hen eggshell powder and synthesized CaO NPs was determined using the Sears method (Yadav, 2012). One gram of adsorbent was mixed with 100 ml of distilled water and 20 gm of sodium chloride. The mixture was shaken for five minutes. Its final pH was adjusted to be 4 with 0.1 M hydrochloric acid. It was then titrated against 0.1M sodium hydroxide to raise the pH from 4 to 9 and the volume (ml) of 0.1M sodium hydroxide used was measured in replicate (repeatedly) and the average value was taken for the specific surface area calculation by sears method.

2.2.4. *Preparation of Adsorbate*

The wastewater contains different pollutants such as dyes, different organic compounds, soluble and insoluble substances, and other metal ions. So it was very difficult to control at the laboratory to treat or to separate these all pollutants. In this case studying the effect of lead (Pb^{2+}) metal ion onto nano CaO alone was appropriate. To avoid the disturbances of other soluble substances that occurred in regular tap or drinking water, distilled water was used to dissolve the metal crystals.

Lead nitrate was helped as the source of the lead stock solution. All the required solutions were prepared with analytical reagents and deionized water. Pb (II)NO_3 was used to give a clear colourless lead solution. According to a preliminary result the equilibrium adsorption of Pb (II) on CaO particle was reached approximately within 105 minutes under the experimental conditions. Accordingly, for all batch adsorption experiments an equilibrium time of 1 hour and 45min was selected.

A lead stock solution with (1000ppm) was prepared by dissolving

1.6146g of 99% Pb $(NO3)_2$ within 1L of distilled water in order to prepare synthetic Pb^{2+} solution as a model pollutant and this was also used to prepare the working solutions with different initial lead concentrations by taking different dilution amounts.

2.2.5. Analytical Methods

For measuring the concentration of lead in the stock solution analytically, and the spectrophotometric determination of Pb^{2+}, chemical 1, 5 Diphenylthio-carbazone (Dithizone) was used. 0.05g of dithizone was dissolved in 100ml of acetone solution. 15 mL of stock solution was taken with 2mL of 3M H_2SO_4 and one mL of dithizone was added. After mixing all this, a cherry red color was formed (Humaira KHAN, 2007). Then in order to know the maximum wavelength of absorbency of the lead solution, 90mg/L of the lead solution was taken and scanned using UV/VIS spectrometer (Lambda 35 PerkinElmer) and it was found that the maximum absorbency (λ_{max}) of lead was 500nm. To calculate the lead concentration from each batch adsorption experiment, a calibration curve was first prepared by using the standard lead solution with known concentrations. Different concentrations were prepared and absorbance values were recorded at λ_{max} of the lead using UV/VIS spectrometer.

2.2.6. Experimental Set Up and Kinetics

Batch adsorption experiments were set for performing all experiments (Figure 2). All experiments were conducted in a conical flask of 250 mL capacity. In each experiment, the solution volume was 100mL. The mixture of solution and the adsorbent were agitated by using a magnetic stirrer on a hot plate at 250 rpm. Initial solution pH was adjusted using a pH meter by dropping HCl or NaOH before adding the adsorbent to the solution. The temperature of the process was adjusted ambient on a hot plate and initial Pb^{2+}ion concentration was taken from synthetic Pb^{2+} ion solution by measuring cylinder. After Adsorption the samples filtered with the help of what man filter papers and the liquid lie above the solid residue was analyzed for Pb^{2+} ion by UV-visible spectrophotometer. Each experiment was performed according to the experimental design layout.

The removal efficiency (E) of the adsorbent can be calculated as (Marandi e al., 2011):

$$\text{Removal efficiency, E (\%)} = 100\ (C_o\text{-}C_t)/Co \tag{2.5}$$

Where, $C_o$and C_t (mg/L) are the initial concentration and concentration at time t of the Pb (II) in the solution, respectively.

Adsorption Kinetics: It is compulsory to realize the rate at which the processes take place and the factors that manage the rate of the processes, for this issue kinetics of the process were evaluated. These experiments were carried out by varying the contact time from 15 to 135 min at ambient temperature, staying other parameters remain constant such as pH, adsorbent dose and initial metal ion concentration at 7, 0.75g, and 60ppm respectively. The samples were shaken at speed of 250 rpm, and withdrawn at 15 minute time intervals to determine the residual of lead ion in the solution. Then data from the experiment was provided into pseudo-first-order model, pseudo-second-order, and intraparticle diffusion (Yuan-dong Huang, 2019).

Adsorption Isotherm: During the solution is contacted with a solid adsorbent, molecules of adsorbate are transferred from the fluid to the solid until the concentration of adsorbate in solution as well as in the solid phase have become in equilibrium. At equilibrium, equal amounts of solute are adsorbed and fluid desorbed simultaneously. This is termed adsorption equilibrium. The equilibrium data at a given temperature are represented by the adsorption isotherm and the reutilization of adsorption is important in a number of chemical processes ranking from the design of heterogeneous chemical reactors to the purification of compounds by adsorption. Adsorption isotherm models like Langmuir, Freundlich, and Temkin, models were used to fit the experimental data. It is used to find the best fitting isotherm model in order to evaluate the efficiency of the prepared adsorbent and to develop a suitable batch adsorber design. The adsorption capacity at equilibrium, q_e (mg/g) was calculated by the equation (2.6).

$$q_e = V\ (C_o\text{-}C_e)/m \tag{2.6}$$

Where q_e are the amounts adsorbed (mg/g) at the equilibrium; C_o and C_e are the concentration of the Pb (II) in the solution (mg/L) at the initial andequilibriumt, respectively; V is the volume of the solution (L), and m is the mass of the adsorbent (g).

Table 1
Design experimental factors and levels used in CCD.

Independent parameters	Coded factors	Coded levels				
		-α	-1	0	+1	+ α
Metal initial concentration (mg/L)	A	30	60	90	120	150
pH	B	1	3	5	9	11
Adsorbent dose (g)	C	0.25	0.5	0.75	1	1.25
Contact time (min)	D	15	45	75	105	135

Table 2
Proximate analysis result.

Parameter	Value in % Raw eggshells	CaO particles Adsorbent
Moisture Content	0.98	0.135
Ash Content	78.2	–
Volatile Matter	2.7	–
Fixed Carbon	18.12	–

2.2.7. Experimental Design

The Central Composite Design (CCD) was used for the optimization of lead adsorption onto CaO particles by applying Response Surface Methodology (RSM) with three levels (M. Bhowmik et al., 2019; S. Ahmadzadeh et al., 2015). It was used to investigate the effects of four factors namely, initial Pb^{2+}ion concentration (A), pH (B), contact time (C), and adsorbent dosage (D) on the response, percentage of Pb^{2+}ion removal (Y)(Table 1, Table 2, Table 6). RSM was used to evaluate the effect of the individual factors, the interaction effects of the variables, and the optimum condition of the responses.The experiments were carried out and data were statistically analyzed by the design-Expert (Stat-Ease, Inc., version 11.1.0.1,) to find the suitable model for the percentage of Pb^{2+}ion removal yield as a function of the above four factors. Design expert software version 11.1.0.1 was applied for analysis of ANOVA and for the optimization of process parameters for adsorption. A central composite design was used to reduce the number of experiments and increase the interaction effect among all factors. From the central composite design we can use the formula:

$$N = 2^K + 2K + n_o \tag{2.7}$$

Where, N stands for number of experinment, k is number of factors and n_o is number of replication. Therefore in this research the number of experiments required were, $N=2^4+2*4+6=30$

Based on the literatures the selected ranges of the factors were pH between 3 to 7, the dose from 0.5g to 1g and the initial metal concentration between 60mg/L and 120mg/L and contact time 45min to 105min.

Development of regression models equations: The Response surface methodology gave the empirical relationship between the response function and the independent variables (factors). The quadratic response model was based on all linear terms, quadratic therms, and linear interaction terms according to the following equation (Bayuo et al., 2019) given by equation (2.8):

$$Y = \beta_0 + \sum_{i=1}^{k} (\beta_i X_i) + \sum_{i=1}^{k} (\beta_{ii} X_i^2) + \Sigma \sum_{i<j} (\beta_{ij} X_i X_j) \quad (2.8)$$

Where, Y= predicted response, β0 = constant coefficient, βi = linear coefficients, βii = quadratic coefficients, βij= interaction coefficients, Xi and Xj were coded values for the factors.

3. RESULTS AND DISCUSSIONS

3.1. Characterization of Adsorbent

Proximate analysis was performed for both raw eggshell and CaO particles adsorbent to analyze its different physicochemical characteristics such as moisture content, ash content, volatile matter, and fixed carbon (Table 2).

The moisture content of both raw eggshell and CaO Particles adsorbent was found to be 0.98 and 0.135 percent respectively. The purpose of measuring the adsorbent moisture content is to identify the adsorbent's better removal capability. The sample's moisture content tells us the percentage of water capacity present in the sample. The percentage of moisture content of both raw eggshell and CaO Particles which were slightly lower than the value reported elsewhere in the literature was 1.174% (BHAUMIK et al., 2012b)). The smaller the percentage of moisture content, the maxima of its adsorption efficiency, as a result, the presence of water in the adsorbent can occupy the adsorbent active sites before it contacts with the solution. Therefore, the adsorption percentage decreased with an increase in the moisture content of the adsorbent (Getasew Ketsela et al., 2020). The ash content is a reflection of the amount of inorganic substituent present and was obtained as 78.2% and this percentage was larger than the ash content of hen eggshell recorded in the former literature 45.29% (Ajala 2018). The higher the ash content values, the higher the quality of the adsorbent for higher removal efficiencies.

Volatile matter is due to the residual organic compounds in the prepared adsorbent and the value of volatile matter obtained in powdered hen eggshell was 2.7%. Since this value is very small, it has no influence on the generated calcinated calcium hydroxide from hen eggshells. Fixed carbon is the combustible solid residue that left calcium hydroxide from hen eggshell was heated then the volatile matter was dismissed. The content of fixed carbon in hen eggshell was calculated by summing the percentage of moisture content, ash content, and volatile matter and subtracting it from total samples. Then the value calculated was 18.12%. Laboratory results of particle densities for both RESP and CaO nanoparticles were 0.98g/cm^3 and 2.01g/cm^3 respectively. This was told us that the particle density of calcium oxide nanoparticles was greater than the raw eggshell powders. The larger the particle density the higher porosity of the adsorbent has resulted. The RESP and calcium oxide nanoparticles bulk densities were 0.719g/cm^3 and 0.375g/cm^3 respectively. From these results, the bulk density of raw eggshells was greater than that of calcium oxide nanoparticles. The greater bulk density the lower porosity of adsorbent has resulted. From those adsorbent studies, the particle density increases from RESP to CaO NPs whereas the bulk density decreased from RESP to CaO NPs and this shows the porosity is low with a high value of bulk density and high with a high value of particle density. From the above particle density and bulk density calculation, the porosity of RESP and CaO NPs was 26.63 g/cm^3 and 81.34g/cm^3 respectively. From the research carried out on activated carbons, there are linear relationships between porosity and adsorptive processes (Aljeboree, 2017). The higher the porosity of an adsorbent had a relatively larger potential for adsorbing the adsorbate. Therefore synthesized Calcium Oxide nanoparticles from hen eggshell had higher porosity than its bulk materials.

FT-IR analyses were carried out to understand the possible interactions between biological molecules and lead ions during the reduction reaction. The FTIR spectrum of CaO nanoparticles was tested to get information about the bending and stretching vibrations of the functional groups. Figure 5 depicts the FT-IR analyses for RESP and CaO NPs synthesized from hen eggshell traveling across numerous bands from 4000-400cm^{-1}. From the figure of RESP, the bands 710cm^{-1}, 876cm^{-1}, 1420cm^{-1}, and 2514cm^{-1} represent the $CaCO_3$, the main component of the RESP, bands 3433cm^{-1} stand for H_2O, bands 2862cm^{-1} and 1796cm^{-1} stands for C=O. As depicted from the figure, both RESP and CaO NPs spectra of carbonate, CO_3^{2-} occur at 876 cm^{-1}. The existence of this band explains the oxygen atom of the carbonate and calcium in the raw eggshells. The sharper band of CaO NPs at 1476 cm^{-1}, 3642cm^{-1}, 876 cm^{-1} and 710cm^{-1} in the figure below shows the stretching of the C-H bond indicating the carbonization of CaO NPs. The adsorption peak at 3642cm^{-1} has resulted because of the O-H bond from water molecules (moisture) on the surface of CaO NPs (Marghiasi et al. 2014). The absence of a sharp band (606cm^{-1}) in the spectra of RESP indicates that the calcium carbonate the main component of hen eggshell was no longer present, it was already converted to calcium oxide nanoparticles. Nearly the consistency of crests for all RESP, CaO NPs, and lead-loaded CaO NPS after the adsorption test was conducted were due to the absorbance of dampness and carbon dioxide from the environment.

Table 3
FT-IR spectral characteristics of CaO NPs before and after Pb (II) ion adsorption.

Functional l groups of IR Adsorption bands	Wave number, cm^{-1} Before adsorption of Pb (II) ion Adsorption bands	After adsorption Pb (II) ion	Shift differences
OH	3454	3447	8
C = C	1639	1629	10
C–C	1476	1463	9
C = O	876	874	2
C–N	1086	1079	7

The FT-IR spectrum of the CaO NPs exposed to Pb (II) ions indicates a decrease in the intensity of the peaks and some shifts or changes in the wavenumbers. Table 3 below depicts the main difference between the wavenumbers before and after Pb (II) adsorption process. The change in the wavenumbers has been predicted by comparing the figure 3 a and b, which were small and less than 10cm^{-1}. This result indicates the possibility that the adsorption process could take place via an ion-exchange process or physical interaction (Blazquez et al., 2010).

X-ray diffraction (XRD) structure analysis of CaO NPs: In order to establish the truth whether the synthesized sample was CaO NPs or not and to investigate the structure of nanoparticles, XRD analysis was behaved and showed good agreement with the standard JCPDF card number 77-2376, the peaks were observed at 2θ=29.3, 32.38, 33.82, 37.4, 54.01, 64.4, and 67.56. The principal peak has appeared at 2θ= 37.4 and the sharp peaks in the XRD pattern reveal the polycrystalline nature of CaO NPs.The result demonstrates that the larger composition in hen eggshell (calcium carbonate) was thoroughly converted to calcium oxide during synthesis. The spherical geometry of calcium oxide was generated during the synthesis of calcium oxide nanoparticles. The crystallite size was calculated by the Debye-Scherer formula and found to be 24.34nm for CaO at FWHM (2θ) of 0.36, which confirmed that the synthesized nanoparticles were nanocrystalline in nature. Figure 4b shows the qualitative phase study of the uncalcined raw eggshell. The analysis for uncalcined eggshell powder revealed the existence of $CaCO_3$, phase as a major component of the sample. All the characteristic peaks observed from figure 4a were fitted with the calcium carbonate phase. The main peak appeared at 2θ=29.55. Through the analysis rhombohedral structure was obtained in this work. A similar result was obtained by (Zaman et al., 2018). Masoud Fouladgar Saeid Ahmadzadeh (2016) also examined the particle size using the Scherrer formula, the average of particles size was obtained as 32 nm.

Thermogravimetric Analysis: The raw eggshell powder decomposition temperature was obtained from the TGA curve. The

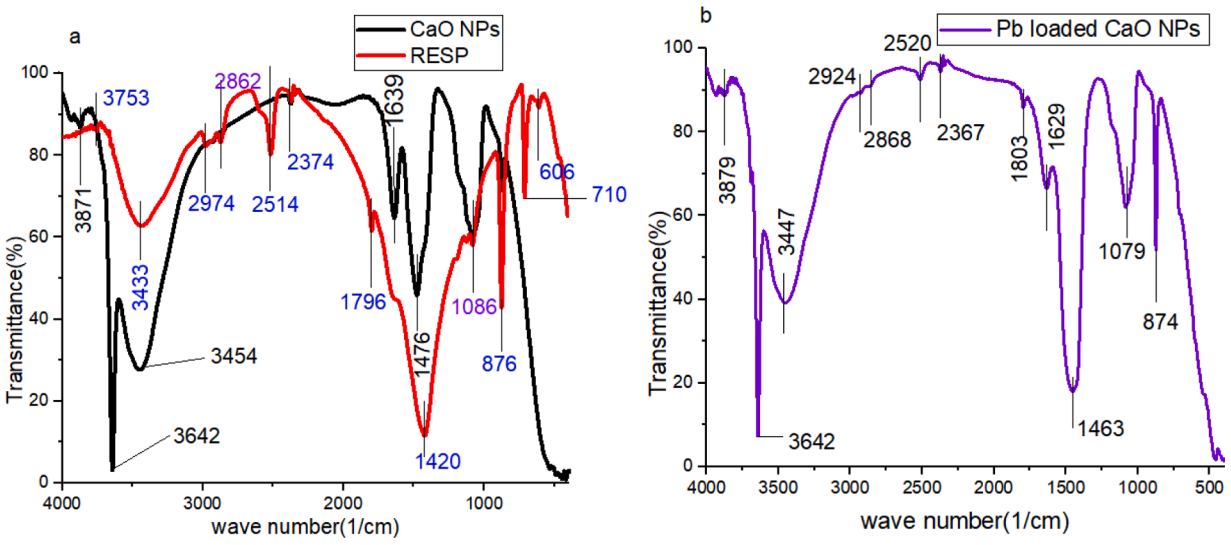

Fig. 3. FT-IR: (a) CaO NPs and RES Powders; (b) lead loaded CaO NPs.

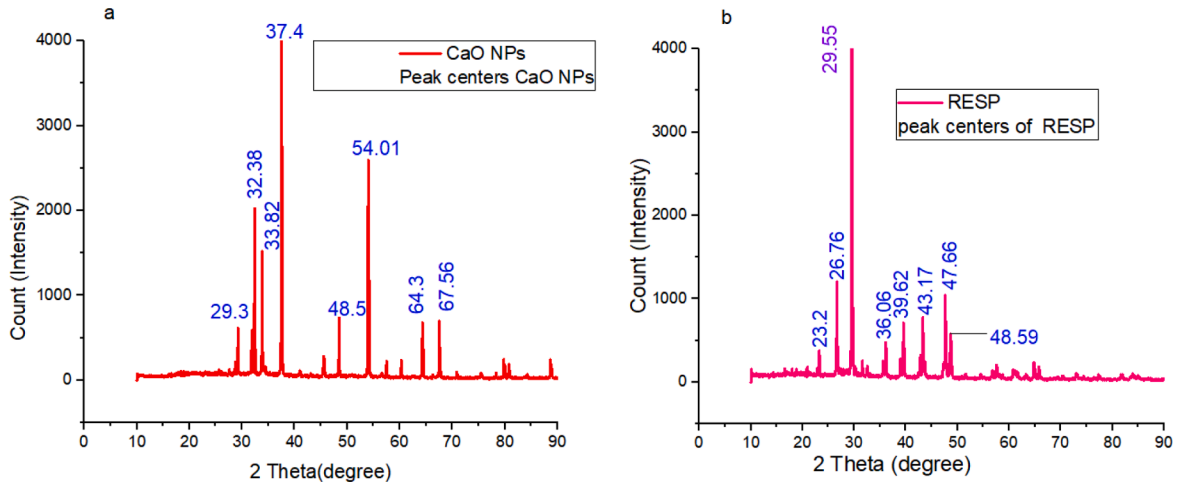

Fig. 4. XRD plot: (a) synthesized Calcium oxide nanoparticles; (b) raw eggshell powder.

thermogravimetric analysis (TGA) of RESP was conducted between ambient temperature and 1000°C in order to determine thermal stability and decomposition temperature. The TGA result showed that significant weight loss was appeared between the temperature of around 600 and 850°C because of removed impurities and the raw eggshell powder residue was stable above 850°C as shown from figure 5a, because CO_2 is released to the environment. In a raw eggshell, a total weight loss of 45.62% was noticed. In the first region of figure 9, the mass loss was related to the loss of volatile substances like water and organic materials. In the second region, the mass loss was due to the release of CO_2 from $CaCO_3$ decomposition.

In the case of Ca $(OH)_2$ gel, prepared from hen eggshell powder as illustrated in figure 5b, the gel was stable or has no significant weight loss above 900°C, and the total weight loss obtained up to 1000°C temperature was 80.4%. But the CaO NPs adsorbent had only a slight weight loss of 4.7% between the temperature of 356 to 385 °C. This amount of weight loss was observed due to the contact of moisture with samples during sample balance and transferred to sample hold up for TG analysis. As illustrated in figure 5c, CaO NPs had high thermal stability and purity. Therefore TG curve of the pure compounds shows the characteristics of the compounds.

Scanning Electron Microscopy (SEM): The morphology and texture of CaO NPs were studied by using SEM. It revealed that the NPs were spongy-like and foamy products with large agglomerates of very small particles. The SEM image of the CaO sorbent sample was shown in figure 6. The surface morphology of the adsorbent particles through investigating the picture/image shows that the synthesized size particles were the lesser size and therefore the adsorbent/sorbent has increased surface porosity with 10μm magnifications. The bright parts of surfaces from the image reveal high emission of electrons when exposed to the electron beam of SEM. This showed the high surface area to volume ratio in the bright parts of surfaces. As it can be observed from the micrograph, the synthesized particles were made of grains with spherical shapes agglomerated from each other. These small particles agglomerated to each other reveal the polycrystalline character of CaO NPs. Other investigations confirmed the spherical shape of CaO NPs (Zahra marghiasi et al., 2014).

The porosity of CaO particles was due to the release of CO_2 from the internal structure, during the calcination of Ca $(OH)_2$. The existence of the developed pores in the CaO microspheres facilitates efficient removal activity of heavy metal from wastewater. Easy separation of heavy metals from wastewater is due to the high surface area, uniformity, and porosity of CaO NPs.

Point of Zero Charge (PHpzc) Analysis: Point of zero charges was formulated by acid/base titrations of a colloidal dispersion of particles in the salt solution. It was crucial to find the point of zero charges (pHpzc)

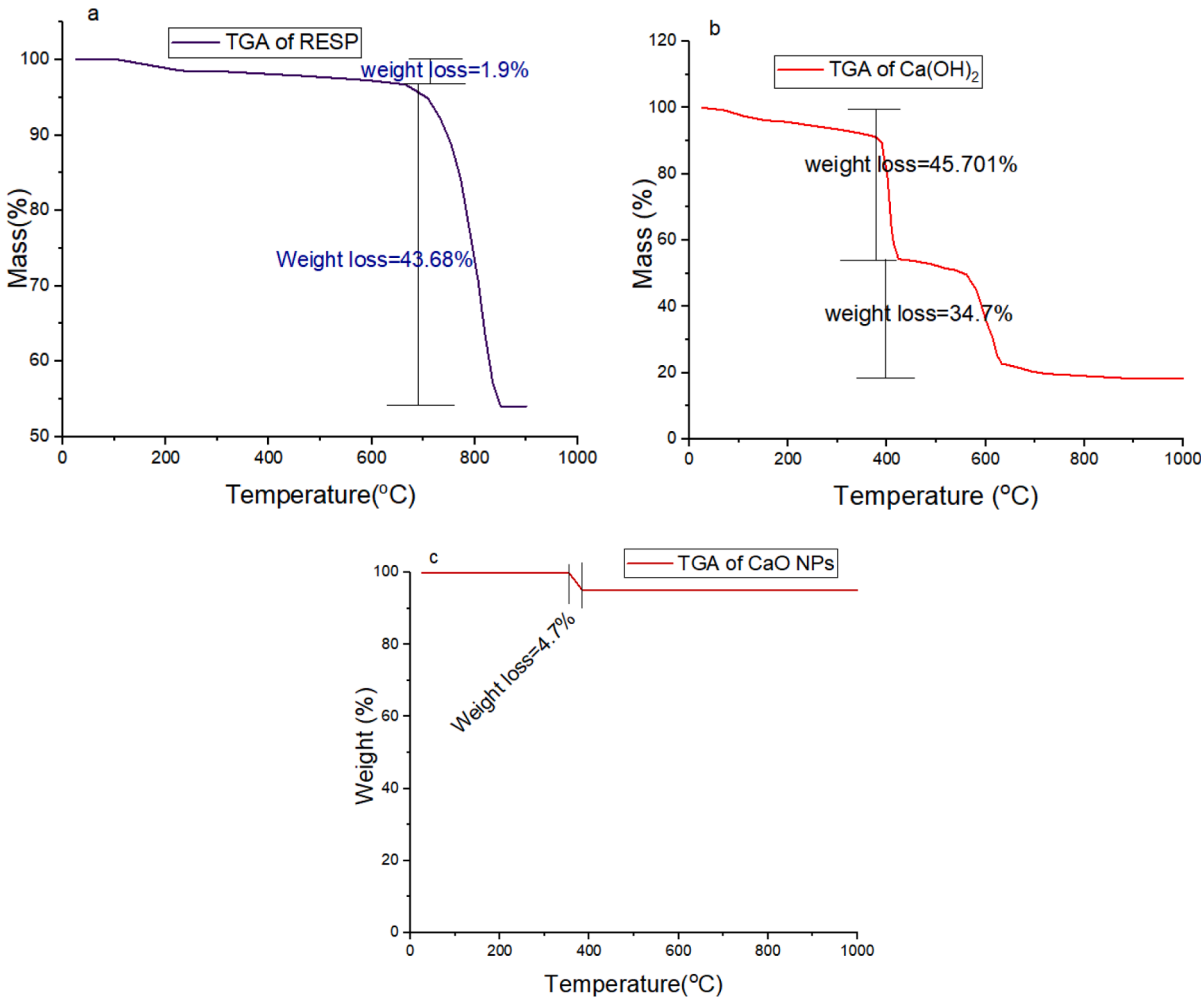

Fig. 5. TGA result: (a) Raw eggshell powder; (b) Ca $(OH)_2$ gel; (c) CaO NPs.

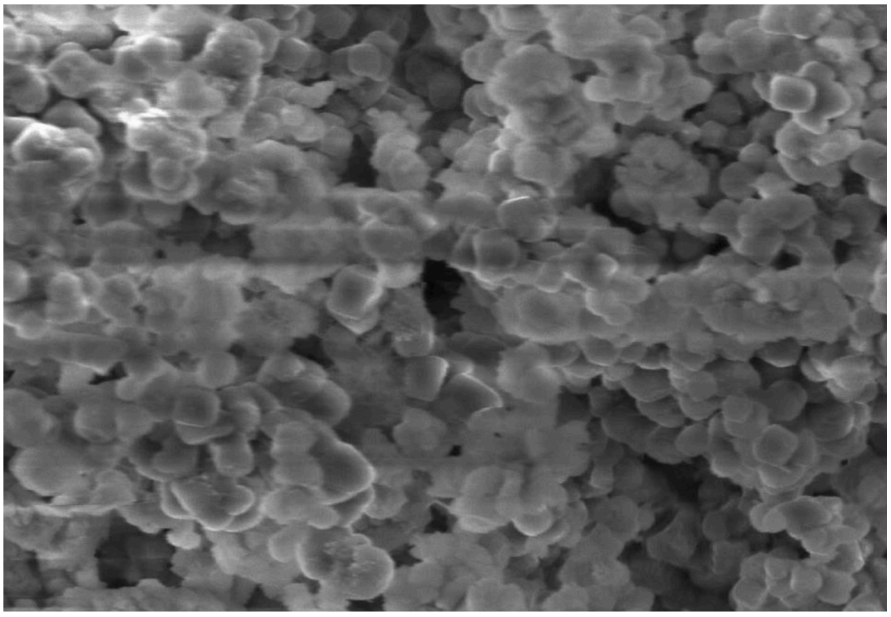

Fig. 6. SEM image of CaO NPs.

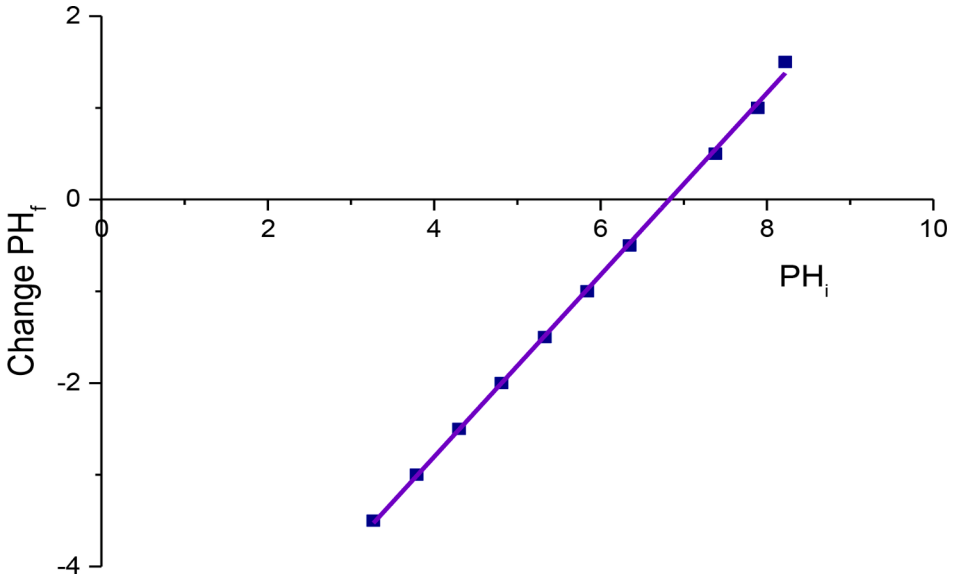

Fig. 7. Zero point charge of CaO NPs.

Table 4
Experimental results of Pb (II) absorption experiments.

Run	Concentration (mg/L)	pH	Dosage (g)	Contact Time (min)	Removal%	Replicate Removal%	Average Removal %
1	120	7	0.5	105	0.196	0.193	0.194
2	60	3	0.5	45	0.232	0.229	0.231
3	120	7	0.5	45	0.265	0.262	0.263
4	30	5	0.75	75	0.072	0.058	0.065
5	90	9	0.75	75	0.125	0.105	0.115
6	90	1	0.75	75	0.426	0.407	0.416
7	150	5	0.75	75	0.358	0.340	0.349
8	90	5	0.75	75	0.116	0.135	0.125
9	120	3	1	45	0.390	0.387	0.389
10	60	3	0.5	105	0.176	0.179	0.178
11	120	7	1	45	0.247	0.243	0.245
12	60	7	0.5	105	0.085	0.081	0.083
13	120	3	0.5	105	0.419	0.415	0.417
14	90	5	0.75	135	0.131	0.113	0.122
15	60	3	1	45	0.173	0.1703	0.172
16	60	7	0.5	45	0.097	0.095	0.096
17	90	5	0.75	75	0.1413	0.1257	0.134
18	90	5	1.25	75	0.162	0.147	0.155
19	90	5	0.75	75	0.129	0.147	0.138
20	120	3	0.5	45	0.512	0.514	0.513
21	90	5	0.75	75	0.147	0.131	0.139
22	90	5	0.75	15	0.258	0.245	0.251
23	60	7	1	105	0.066	0.063	0.065
24	90	5	0.25	75	0.281	0.263	0.272
25	120	7	1	105	0.173	0.176	0.175
26	60	3	1	105	0.129	0.125	0.127
27	60	7	1	45	0.092	0.088	0.090
28	90	5	0.75	75	0.122	0.141	0.131
29	90	5	0.75	75	0.121	0.124	0.123
30	120	3	1	105	0.306	0.308	0.307

of the adsorbent to investigate the surface behavior of the adsorbent, and the influence of pH in the adsorption process. When pH < pHpzc, the surface charge on the adsorbent is a net positive charge and when pH>pHpzc, the surface charge on the adsorbent is a net negative charge. Therefore, anions adsorption on the surface of the adsorbent is favorable at a pH value lower than PHpzc, and cations adsorption on the adsorbent surface is favorable at a pH value higher than PHpzc. From the figure below the point of zero charges obtained from the experimental results was pH 6.82 this was greater than pH 6.3 which was reported in the literature (R.Bhaumik et al., 2012).

The CaO NPs adsorbent works best at the cationic molecules of acidic surface charge. Therefore this indicates that cation adsorption was enhanced at 6.82< pH, hence pH of greater than 6.82 (pH>6.82) was preferable for cationic adsorptions. Therefore, the adsorption of the Pb (II) was favored at pH greater than the pH_{PZC} where the surface of the adsorbent becomes negatively charged.

Graphical illustration (figure 7) indicate that pH value kept greater than the obtained pHpzc, 6.82 to make a powerful negatively charged surface which causes electrostatic attraction between a molecule of adsorbate and adsorbents. Less than this pH, the surface charge of the adsorbent gets positively charged because of the protonation of functional groups which make H^+ ions which compete well with Pb cations, these results a decrease in the expected amount of adsorbate adsorbed. In general adsorption of the cations increases with increasing pH,

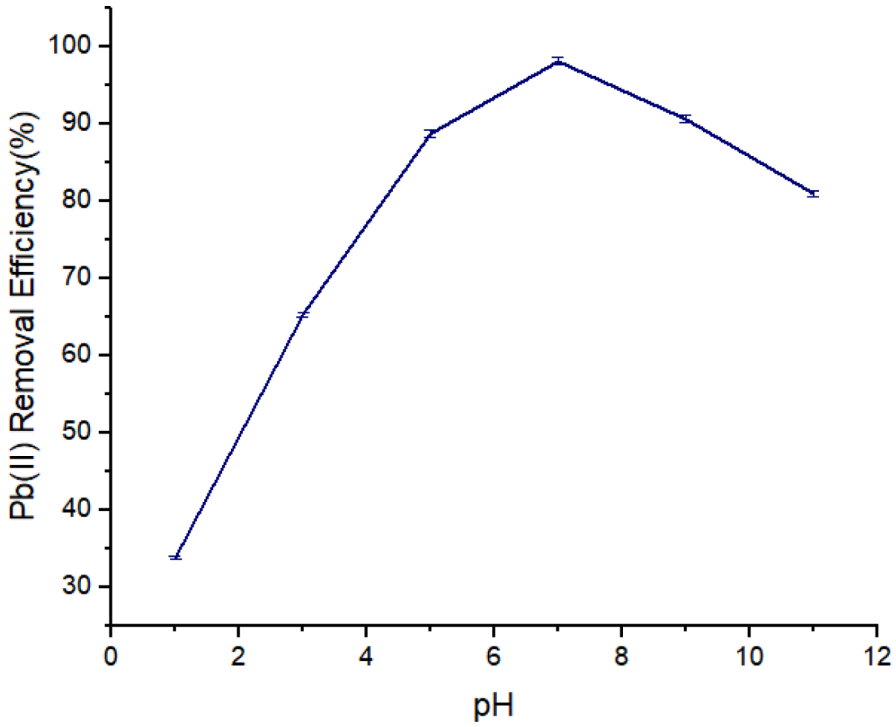

Fig. 8. Effect of pH on Lead (II) removal.

whereas adsorption of anions increases with decreasing pH.

Determination of Specific Surface Area: As described under material and method, determination of surface area was calculated. The titrated volume using NaOH to raise the pH of the solution from four to nine were 1.95 and 3.2ml RESP and CaO NPs respectively. The specific surface area of RESP was 37.4 m^2/g, this was greater than 21m^2 /g (Viriya-empikul et al., 2012). The CaO NPs surface area was 77.4 m^2/g. From this titration experiment synthesizing nanoparticles adsorbent and calcination process increases the specific surface area of the adsorbents. In general, the larger the specific surface area of the adsorbent, the better is the adsorption performance.

3.2. Pb (II) absorption studies

At the end of the lead absorption study, the residual/suspension was separated through filtration processes. After filtration; the lead

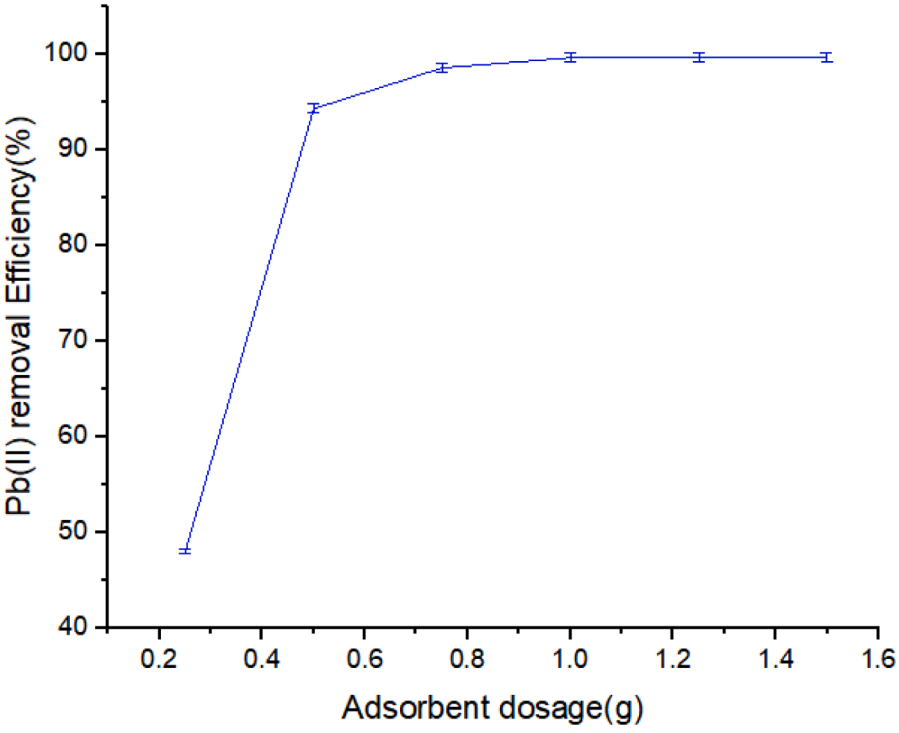

Fig. 9. Effect adsorbent dosage on Pb (II) removal.

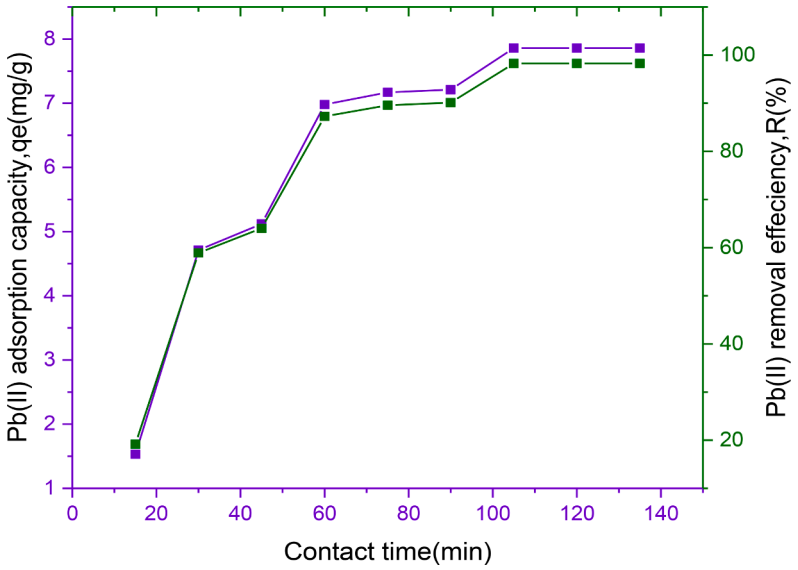

Fig. 10. Effect of contact on Pb (II) removal.

concentrations were determined by UV-spectrophotometer. All 30 run experiments were done with different combination of four parameters and the values were recorded as illustrated in Table 4.

3.2.1. *Effect of PH on Pb (II) Removal*

The adsorption of lead (II) from an aqueous solution using CaO nanoparticles using in this research was highly dependent on the pH of the solution. The graph illustrated in figure 8 indicated that the removal percentage of Pb (II) increased with increased pH. Solution pH dependency of metal uptake is related to both surface functional groups on the surface of the adsorbent and the metal chemistry of the solution (M. Bhowmik et al., 2019). This was because the point of zero charges of the calcium oxide nanoparticles was at 6.82. The positively ionic adsorption process is preferred at pH greater than the pH point of zero charges. Lower Pb (II) removal efficiency was noticed at 33.83% at pH 1 and higher Pb (II) removal efficiency was 98.12%. At lower pH, H_3O^+ ions compete against Pb^{2+} ions for binding and are surrounded by hydronium ions (H^+) stopping metal ions from approaching the binding sites and it leads to low adsorption capacities.

Positively charged metal ions and positively charged sites were incapable of binding metal ions due to electrostatic repulsion. Because of this, low removal percentage of Pb^+ was observed. There were fewer H^+ ions taking place in the solution when pH increased and as a result more negatively charged sites were made and higher metal ion removal was introduced by electrostatic attraction. In alkaline conditions of pH greater than 7, the removal efficiency was reduced. This is because at low pH (<7), positively charged Pb (II) species are dominant and adsorption on CaO NPs takes place at a faster rate. But in the case of pH

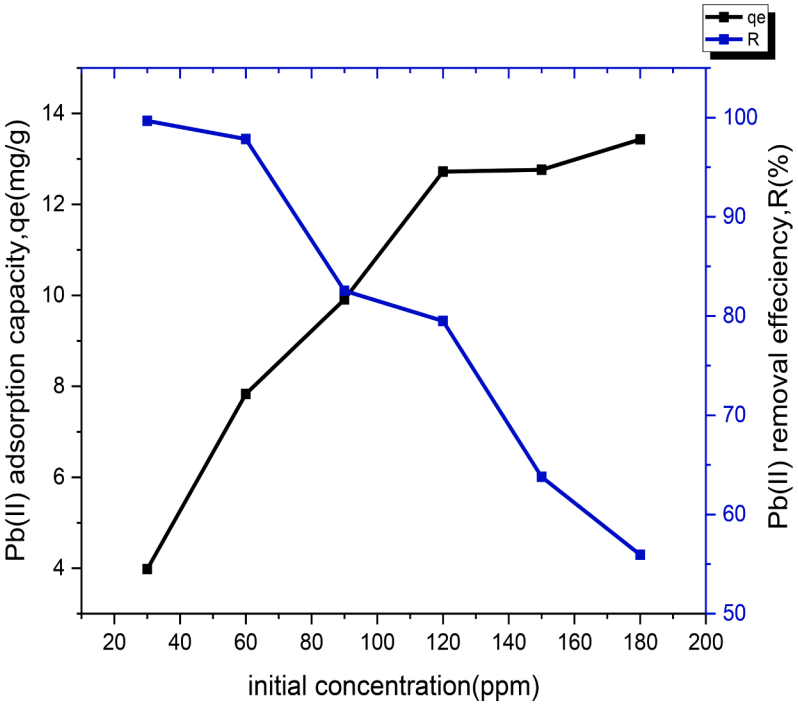

Fig. 11. Effect initial concentration on lead (II) adsorption.

Table 5
Langmuir separation factor, R_L and Summary equilibrium constants and parameter values of Pb (II) with different isotherms.

Concentration (mg/L)	Langmuir Separation factor, R_L of Pb
30	0.022
60	0.011
90	0.0074
120	0.0056
150	0.0045

Summary of different isotherms

Heavy metal ion	Langmuir isotherm			Freundlich isotherm			Temkin isotherm		
	Qm (mg/g)	K_L (L/mg)	R^2	n	K_f (mg/g)	R^2	K_T (mg/L)	b_T (J/mol)	R^2
Pb as total	0.877	1.48	0.996	5.455	6.5203	0.978	176.69	1773.73	0.977

values (pH>7), the adsorption was reduced due to different production of lead species with different charges like Pb (OH) $^{+}$, and Pb $(OH)_2$ (Gupta VK, 2004). However, the efficiency of the processing process is insignificant Due to the formation of oxonium ions, it decreases when the pH drops below 3. Limits the formation of hydroxyl radicals (Dolatabadi et. Al., 2021b). Rezayi M et al., (2014) studied that at higher pH values (5 and above), the formation of titanium oxide precipitates moving out of solution significantly alters the potential response of the electrodes.

3.2.2. Effect of Adsorbent Dosage

The effect of CaO NPs dosage on the adsorption of Pb (II) ion in aqueous solution was studied by varying the CaO NPs sample from 0.25g to 1.5g for constant initial concentration, solution pH, and contact time, 60mg/L, 7, and 105min respectively. The adsorption increased as adsorbent dosage of CaO NPs increased. With increasing CaO NPs adsorbent dosage, the binding sites or available surface area for adsorption increases, and it leads to the increasing of Pb (II) removal efficiency at neutral pH, 105 min contact time and 60mg/l initial concentration of Pb (II) ion. As depicted in figure 9, more than 99.67% removal of Pb (II) with 1g/100ml dose of adsorbent after 105min contact time. No significant change was observed in the removal of lead (II) when the dose of an adsorbent is increased beyond the optimum dose. The increased in adsorbent dosage with increase adsorption efficiency is because of the increase in adsorbent binding sites and a similar effect is investigated by (Zhang, 2012).

3.2.3. Effect of Contact Time

The effect of contact times (from 15 to 135min) of the removal of Pb (II) is shown in figure 10. From the obtained results, it was observed that the percentage removal of Pb (II) ion and adsorption capacity increased sharply with an increase in contact time of the first 105min and a similar result was investigated in the literature (Moo-Yeal et al., 2017). As depicted in figure 11, it could be concluded that as contact time increases the removal efficiency and metal adsorption capacity increases up to equilibrium was reached at 105min. Further increase in contact time beyond 105min did not enhance the Pb (II) removal efficiency and the adsorption capacity.

3.2.4. Effect of initial metal concentration

Adsorption experiments by variation of initial concentrations ranging from 30 to 150mg/L were carried out with a fixed dose of adsorbent, solution pH, and contact time, 0.75g, 7, and 105min respectively. This result showed that the removal of Pb (II) percent decreased as the initial concentration of Pb (II) was increased. Lead (II) removal ranked from 99.66% to 63.8% at initial Pb (II) concentration of 30 to 150mg/L as shown in figure 11. This behavior could be happened due to the limitation of active sites on the adsorbent surface. At higher concentrations, the metal ions are relatively higher than the available binding sites, hence, decreasing the removal percentage.

This plateau represents saturation of active sites found on CaO NPs samples for interaction with contaminants illustrating those less favorable sites was involved in the process with increasing concentration. Another reason for percentage removal decreased was in the equation %R= $(C_O\text{-}Ce)/C_O$ larger increment in the denominator when compared with the numerator value. But as initial metal concentration increased the adsorption capacity of Pb (II) was increased. This was due to the increased driving force of mass transfer between aqueous solutions of metal ions and the solid adsorbent.

Table 6
Kinetics Parameter's values.

Kinetics model	Parameters	Values	Correlation coefficients
Pseudo first order	qe (mg/g)	18.34	
	K_1 (min^{-1})	0.0496	R^2=0.945
Pseudo second order	qe (mg/g)	13	
	K_2	0.0011	R^2=0.908
Intra particle diffusion	Ki	0.75958	R^2=0.928
	C	- 0.05538	

3.2.5. Experimental results on Adsorption Isotherm

The adsorption isotherm is typically described by an isothermal equation whose parameter expresses the affinity, and the surface property of the adsorbent. The adsorption isotherm can be generated based on the theoretical models from which Langmuir, Freundlich and Temkin models are the most used. They study the relationship between the adsorbate on the surface of the adsorbents that is the number of species adsorbed per unit mass of adsorbent and concentration of solute left in the solution. The possibilities of the adsorption isotherm which describe the resulted data depend on the correlation coefficients (R^2).

Those adsorption data can be interpreted using the relationships which describe the distribution of Pb between aqueous solution and solid phases. These three isotherm models relate metal uptake per unit mass of adsorbent, q_e, to equilibrium adsorbate concentration in the bulk fluid phases, Ce. The linearization of these three isothermal models was used to check the best fitting model. Langmuir models fitted to the sorption data very well in the investigated concentration range with a maximum correlation coefficient of R^2 value 0.9963 as depicted in supplimentary file figure S2. The Langmuir model assumes that the adsorptions of metallic ions occur on a homogeneous surface by monolayer adsorption where interaction between the adsorbed ions (molecules) was negligible. The Langmuir constants like K_L and q_m were calculated from C_e/q_e versus C_e and obtained as 1.48mg/L and 0.877mg/g respectively. A separation factor can be calculated as $R_L = 1/(1+K_LC_O)$, value occurred between 0 and 1.0 which clarify favorable adsorption as shown in Table 5 (Yusuff et al., 2017). If $0 < R_L < 1.0$ it represents favorable adsorption; if $R_L > 1.0$ it represent unfavorable adsorption and if $R_L = 0$ it represents irreversible adsorption. Das et al., (2020a) also studied adsorption kinetics according to a pseudo-secondary kinetics model with the additional effect of intra-particle diffusion. The linear fit of the isotherm model followed the Langmuir isotherm with an equilibrium adsorption capacity of 175.44 mg / g at room temperature. Deb et al., (2019) also stated that, both MO

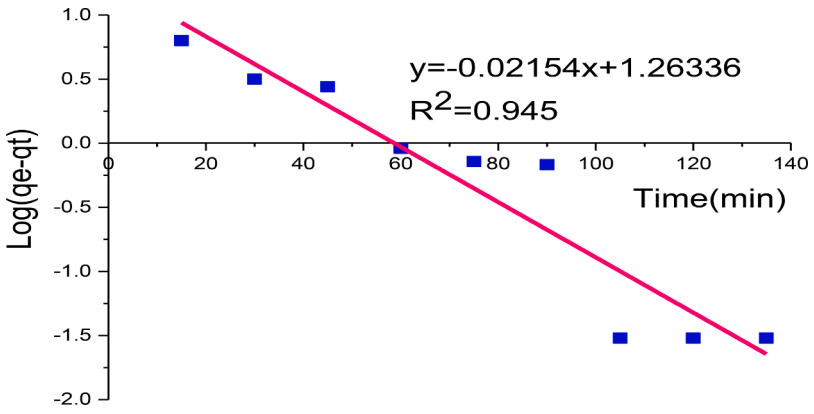

Fig. 12. Pseudo-first-order kinetic model of Pb (II) adsorption.

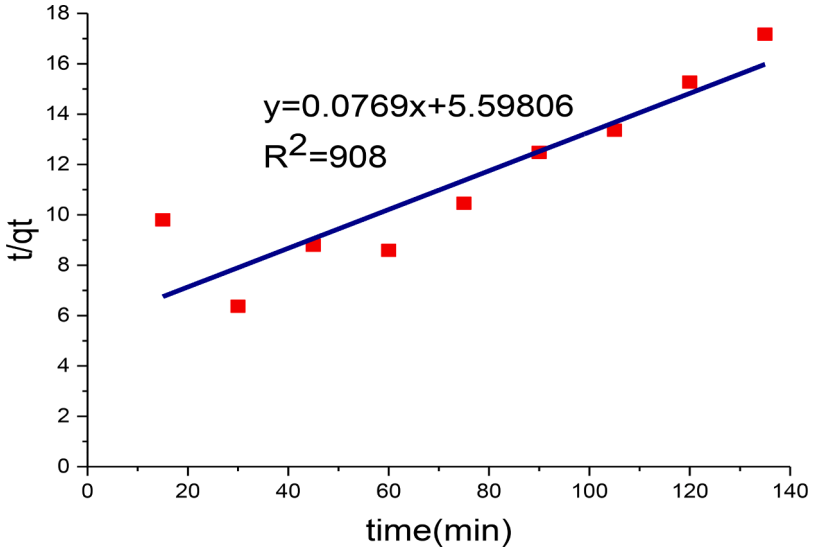

Fig. 13. Pseudo-second-order kinetic model graph of Pb (II) adsorption.

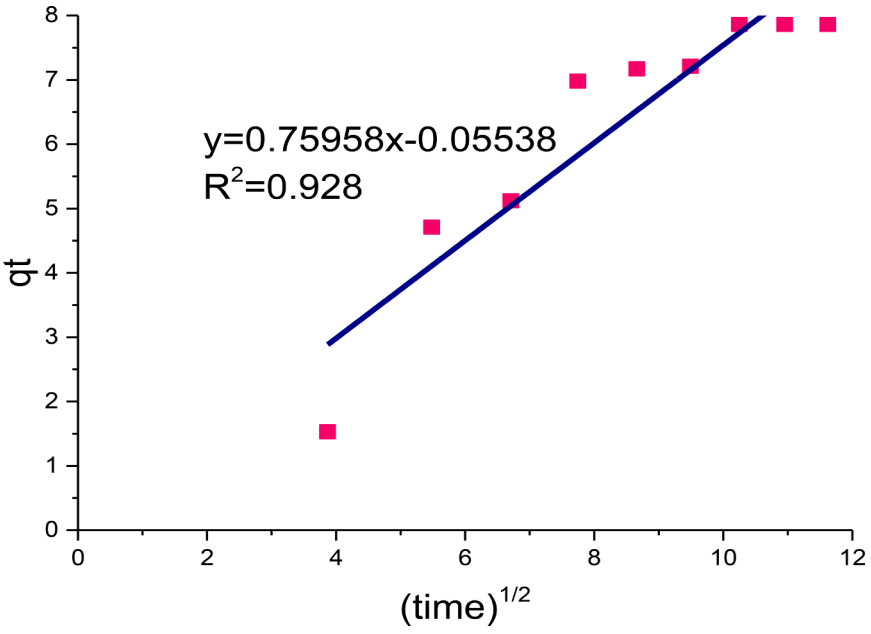

Fig. 14. Intra particle diffusion kinetic model for Pb (II) adsorption.

and EY Experimental data on dye adsorption closely follow Langmuir's isotherms. Maximum single-layer adsorption capacity of 126.58 mg / g and 112.36 mg / g observed with MO and EY dyes, respectively.

The Freundlich isotherm was an empirical modeling equation used to describe heterogeneous systems. The model was plotted as log Ce against log qe as depicted in supplimentary file figure S3, to get the values of constants K_F and n indicating the adsorption capacity and the adsorption intensity. The Freundlich constants K_F and n were 6.52034mg/g and 5.455 with the correlation coefficient obtained being R^2=0.978.

A graph of qe against ln Ce shown in supplimentary file figure S4 was to check the validity of Temkin isotherm and to obtain the equilibrium constants K_T and b_T. Where constant b_T describes the heat of adsorption (J/mol) and K_T is equilibrium binding constants (L/mol) stands to the maximum binding energy. The correlation coefficient obtained from the graph of Temkin was 0.977 which was smaller than the correlation coefficient obtained from Langmuir and Freundlich isotherms. And from those Langmuir isotherm scored the highest correlation coefficient (R^2) and well fit the isothermal model.

A similar result was investigated using copper oxide nanostructure with oval-shaped (Farghali et al., 2013). Therefore, it could be concluded that the Langmuir isotherm model is more suitable for adsorption of Pb (II) ions than the Freundlich and Temkin isotherms based on experimental study.

3.2.6. Kinetic Study

To study the adsorption kinetics of lead (II) heavy metal ion, various kinetic models such as pseudo-first-order, pseudo-second-order, and intraparticle diffusions were under considerations and the kinetics parameters (variables) such as the adsorption capacities, the kinetic models, and their respective correlation coefficients were calculated from the slope and intercept of their curves. The linearized pseudo-first-order kinetics curve of ln (q_e-q_t) against time shows the relevance of this kinetics model as depicted in figure 12. K_1 and q_e values can be determined from the slope and intercept of the schematic plot respectively.

The values of K_2 and q_e were calculated from graph of t/q_e against t conforming intercept and slope respectively as shown in figure 13.

If a plot of qt versus $t^{1/2}$ is linear and passes through the origin, then the intraparticle diffusion is the only rate-limiting step. However, as figure 14 illustrated the linear graph did not pass through the origin. Even though intraparticle diffusion has participated in the process of adsorption, it was not the only rate-limiting step.

The pseudo-first-order model provided the highest correlation coefficient and the model adequately represenst the experimental kinetic data, whereas the pseudo-second-order model provided in contrast the lowest correlation coefficient (Table 6). This shows that the rate-limiting step in lead (II) adsorption process onto CaO NPs is chemical sorption including valence forces through the exchange of electrons between sorbent and sorbate. Das et al., (2020b) also reported that, In the meantime there is an R^2 value for the MR dye 0.905-0.987 and 0.999-1.000 for pseudo-primary Each is a pseudo-secondary kinetics model. Similarly, the R^2 value of the CR dye is intermediate. 0.889-0.966 and 0.999-1.000 for pseudo-primary Pseudo-secondary kinetics model, respectively. A Deb et al., (2020) was mentioned that, the adsorption of EBT dyes on PAn / ZnOPNC strictly follow a second-order pseudodynamic model. Valence force or electron exchange (chemisorption)

3.3. Statistical and Graphical analysis of experimental results

3.3.1. Analysis of Variance (ANOVA)

Analysis of variance (Supplimentary file Table S1) was used to evaluate the significance of the quadratic model. The application of design expert software was to design the experiments, and randomize the runs. Randomization makes the process parameters (factors) in one run neither depend on the process parameter of the previous runs nor predict the conditions in the subsequent run. The different process parameters such as initial metal concentrations, solution pH, adsorbent dosage, and contact time in the adsorption percentage of Pb (II) were generated in the model and optimized by response surface methodology.

Adequacy and significance of the quadratic model were determined by analysis of variance (ANOVA). It was found that the model was statistically significant at the F-value of 246.08 and the value of (Prob >F) <0.05. The parameters which have F-probability of statistics value less than 0.05 were always significant. From this current study, the probability of model F statistics was <0.0001 illustrating that the model suggested by the software was highly significant. In this case, A, B, C, D, BC, BD, A^2, B^2, C^2, D^2 were statistically significant (P<0.05). The p values greater than 0.1000 indicate the model terms are not significant.

The lack of Fit F-value of 2.01 implies it is not significant relative to the pure error. The non-significant value of lack of fit for the model implies that the developed model is valid. It is concluded that, the smaller the P-values and the larger the F-value the more significant is the corresponding models and regression coefficients. The values of Prob >F< 0.05 indicate a significant regression at a 95% confidence interval.

The regression coefficient and the corresponding confidence interval 95% (CI) interval low and high was depicted in supplimentary file Table S2. If zero (0) was in the list of low and high 95% CI, the factors have no effects. Therefore, from the below table it could be judged that the regression coefficients of initial concentration, pH, dosage, contact time, and the combined effects of all have a highly significant effect on Pb (II) adsorption process.

The determination coefficient of (R^2) was used to check the accuracy of the model. The determination coefficient (R^2=0.9957) revealed that the model cannot explain only 0.43% of the total variable. From Table 7, the R^2 of 0.9957 was in reasonable agreement with the Adjusted R^2 =0.9916, their difference was less than 0.2. The regression coefficient (R^2) quantitatively examines the relatedness between experimental and predicted responses. Results of R^2=0.9957 and Adj-R^2 =0.9916 resulted explain that the predicted values were found to be in good agreement with the experimental values. Seeing that the R^2 value is nearer to one, it shows that the regression line exactly fits the data. Generally, the model's best fit was checked by regression coefficient (R^2) and it also suggests a good adjustment to the experimental results. The adjusted determination coefficient, Adj-R^2= 0.9916 was adequate for proving the significance of the model. Predicted-R^2 indicates that the model explains a high percentage of 0.9788 of variability. Model precision gives the ratio of the signal to the noise. The ratio determined was greater than 4 is desirable and the Adequate precision of 59.2981 indicates an adequate signal. This model can be used to navigate the design space. A low value of the variation coefficient (CV=2.97) shows the reliability of the experiments.

Table 7
Model adequacy measures.

STD. Dev.	2.05	R-Squared	0.9957
MEAN	69.07	ADJ R-Squared	0.9916
C.V. %	2.97	PRED R-Squared	0.9788
PRESS	310.16	ADEQ Precision	59.2981

Final equation in terms of coded factors:-

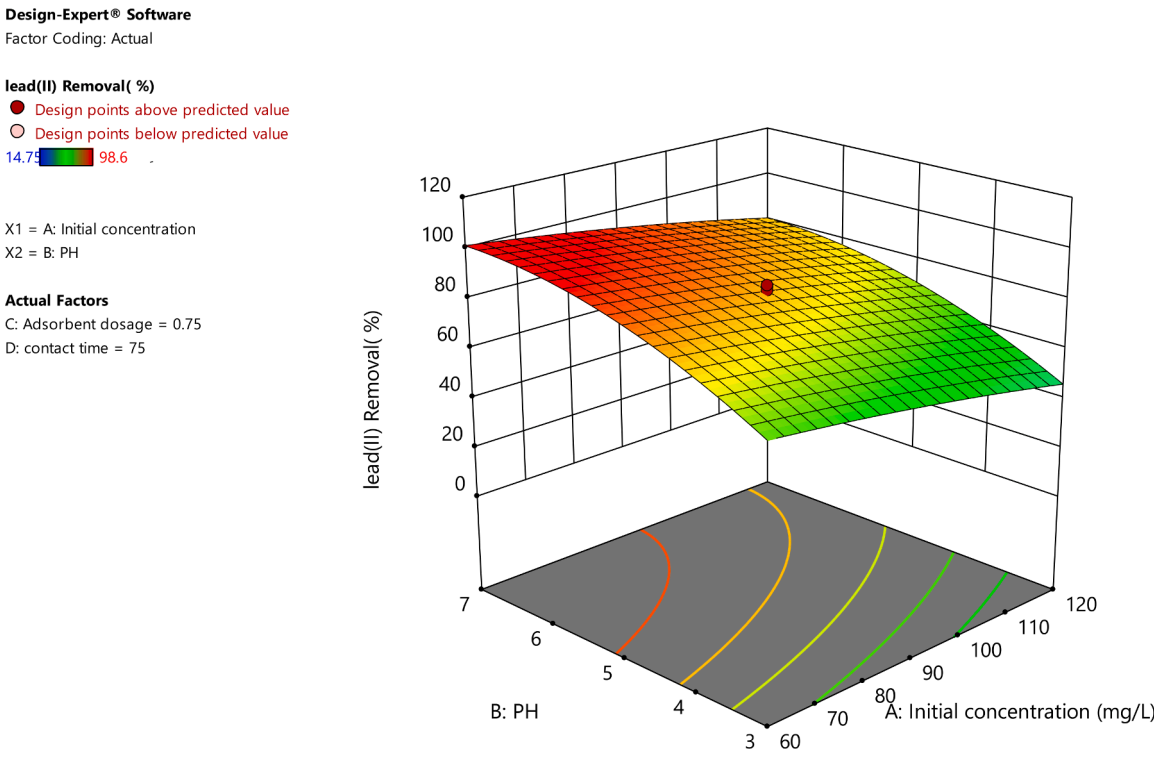

Fig. 15. Combined effect of pH and initial concentration of Pb (II) removal Response surface plot.

$$\begin{aligned}\text{Pb(II)\%Removal} = {} & 83.57 - 10.18 * A + 17.32 * B + 6.40 * C + 7.01 * D + 0.050 * A * B \\ & +0.1113 * A * C + 0.5550 * A * D - 4.23 * B * C - 1.83 * B * D - 0.1312 * C * D - 1.53A^2 \\ & -8.17 * B^2 - 5.01 * C^2 - 3.40 * D^2\end{aligned} \quad (4.1)$$

The equation (4.1) describes how to lead metal adsorption onto sol-gel based synthesized CaO NPs was affected by individual variables (linear and quadratic) or double interaction. Those negative coefficient values show that individual or double interactions factors negatively affect lead (II) adsorption while positive coefficient values represent the factors that increase Pb (II) removal efficiencies. From the equation above, among all linear factors, initial metal concentrations had a negative effect, but pH, adsorbent dosage, and contact time had a positive effect on lead removal. Therefore positive values favored the optimization of the process conditions.

From the table below, the output of different model summary statistics emphasis the model maximizing the predicted R-squared and adjusted R-squared values large, and so the second-order polynomial was suggested by the software.

3.3.2. Graphical Analysis of one factor and interaction effects on ANOVA

Model diagnoses are the graphical plot of summaries for the case statistics and the summary of statistics shown in supplimentary file Table S3. It is usually important to check the fitted model to ensure an adequate approximation to the real system. Different diagnostic models plotted were a normal probability plot which compares the distribution of residuals along a straight line (the normal distribution).

Tolerate some scatter even if with normal data. Focus only on definite patterns like an S-shape curve, which indicates the transformation of responses may provide a better analysis. The residuals versus predicted plot checks for constant variance across the ranges of prediction. Variances that are not constant are indicated as upward or downward patterns. If the plot has randomly scattered between red lines and then the assumption of constant variance is confirmed.

The predicted versus actual from Supplimentary file figure S5, indicates that all the data points were distributed along the 45° line, indicating that the model can provide an acceptable fit for experimental data. Similar results are obtained by (Okolo et al., 2020). Normal plot versus residuals in Supplimentary file figure S5, used in judging whether the models are satisfactory. The figure indicated that the data were plotted against a theoretical normal distribution, and the points should form an approximately straight line and a departure from this line would indicate the departure from a normal distribution. From this graphical result, the data points were very small deviating from the normal distribution given, but not very critical. From the plot shown in Supplimentary file figure S5 the normal probability plot indicates the predicted followed by actual value distribution, in the case of experimental data the point in the plot shows fitted to the straight line. This shows both the actual experiment and the predicted values were approximate and the model satisfies the assumption analysis of variance (ANOVA) i.e. the error distribution was approximately normal. The plot of the residuals versus the predicted was used to examine the reliability of the model, as illustrated in Supplimentary file figure S5. From the graphical result, no series of increasing or decreasing points of the patterns such as increasing residuals with increasing fits and of a predominant of positive or negative residuals should be found which is chance met in my work. The plot of the residuals against the run was used to examine the reliability of the model, as indicated in Supplimentary file figure S5. The figure showed the data points were scattered randomly and do not form a trend, but almost all the data points in the plot were within the boundaries marked by the red lines. Therefore, there was only one

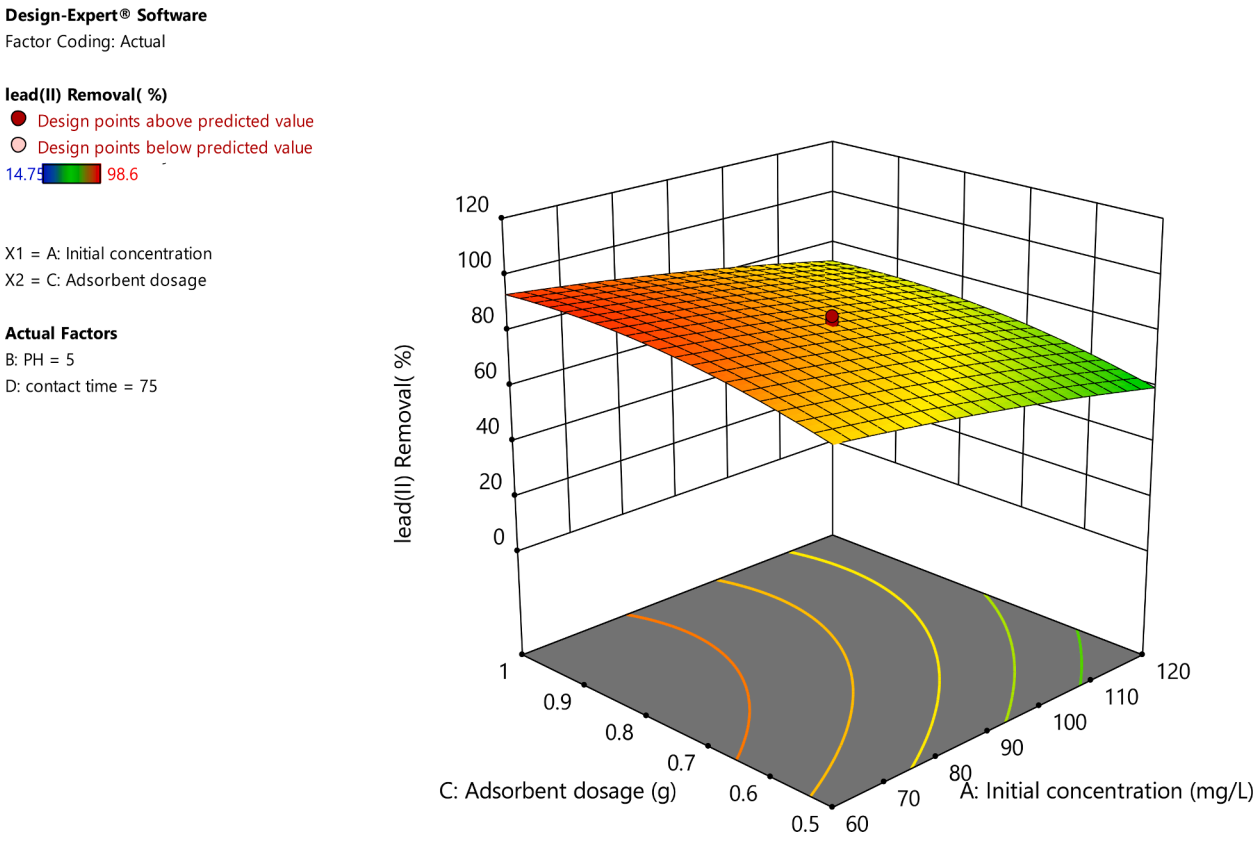

Fig. 16. combined effect of initial concentration and adsorbent dosage on Pb (II) removal response surface plot.

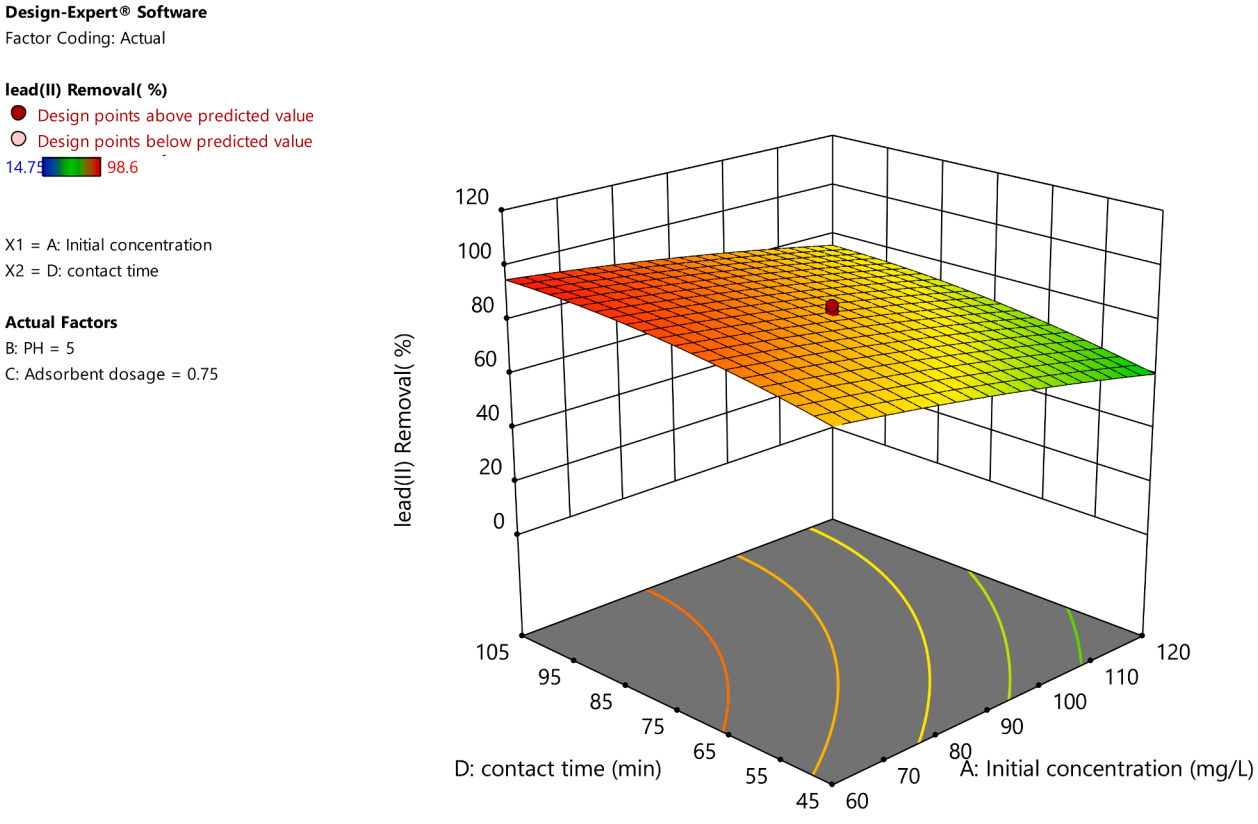

Fig. 17. Combined effect of initial concentration and contact time on Pb (II) removal A) 3D Response surface plot B) Contour plot.

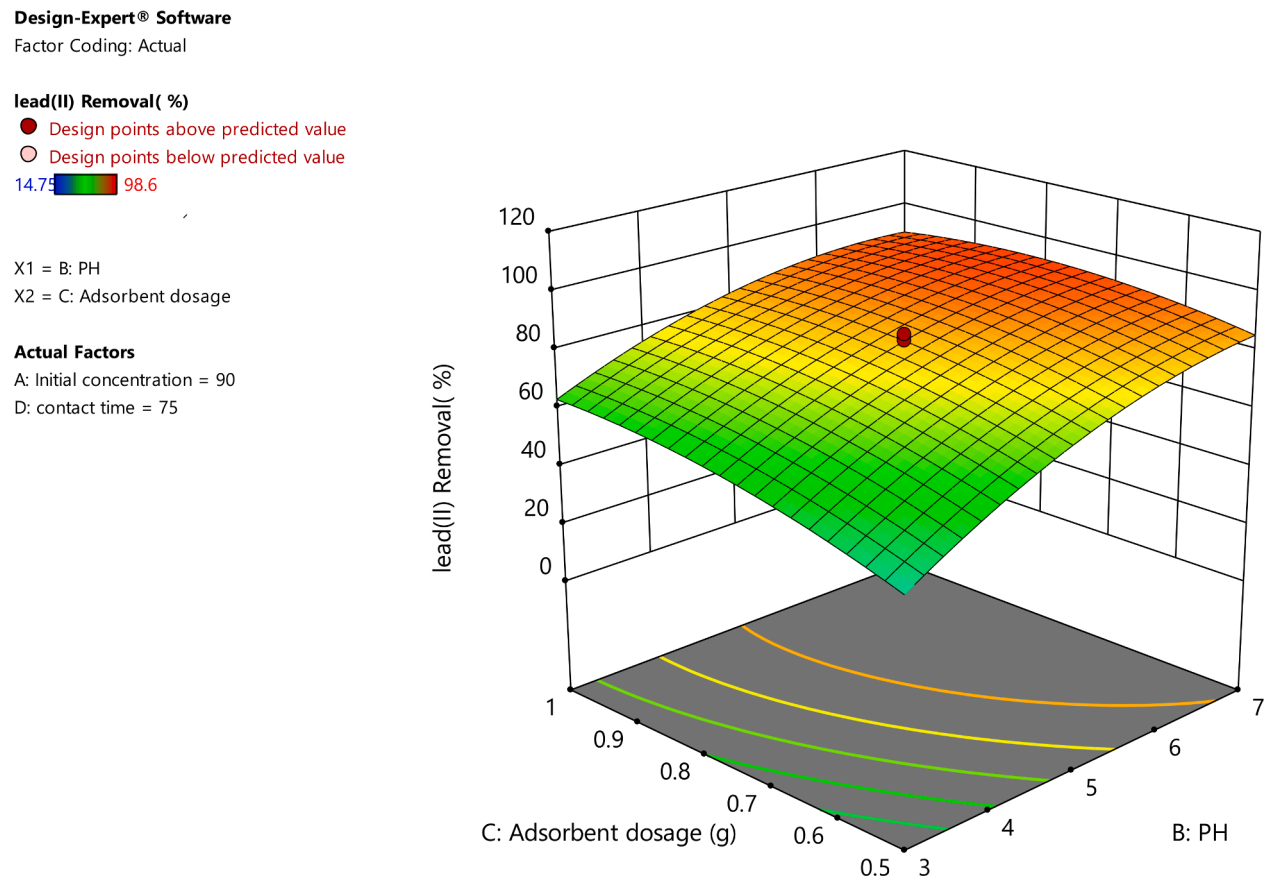

Fig. 18. Interaction effects of pH and adsorbent dose of Pb (II) removal: response surface plot.

outlier data.

If the model is correct and the assumptions are satisfied, the residual should be structured less. It is also unrelated to any other variables including the predicted response. A simple check is to plot residual versus predicted (fitted) values. A plot of residuals versus the rising predicted response value tests the assumption of constant variances. The plot shows random scatter which indicates no need for an alteration to minimize personal error.

3.3.3. Estimation of the quantitative effects of the factors

The objectives of the CCD method applied in this study were to find out the significant effect of the process variables on the percentage removal of Pb (II) on 3D response surface and contour plots and were used to study the effect of all factors on the response. Model Analysis of response surface plot and contour plot was the graphical representations of the regression equations used to study the relationship between the response and experimental levels of each factor.

There were two effects, single (main) and interaction effects which were studied by using a design expert graph. The single effects in the linear model are furtherly studied by considering one-factor change within a range beginning from lower level to higher level, making the other factors at the medium level (center point). As it was illustrated in Supplimentary file figure S6, the removal percentage of lead (II) ions decreased with increasing initial concentrations. The maximum percentage removal, 79.558% was obtained at 60mg/L, and the minimum percentage removal, 58.78% was obtained at 120mg/L. For pH, minimum reduction percentage, 51.81% resulted at pH=3 and maximum removal percentage, 86.5% has resulted at neutral pH. This is because as pH increases, the adsorbent surfaces become less protonated and stronger attraction of cationic species of Pb (II). In the acidic pH, the most common species of Pb (II) cation were: Pb^{2+}, $Pb(OH)^{+}$ and $Pb(OH)^{2+}$, hence under acidic conditions the adsorbent's surface becomes protonated, consequently there is a decrease in the electrostatic attraction between Pb (II) and the surface of the adsorbent, with a decrease in adsorption percentages (Okolo et al., 2020; Rounagh et al., 2009).

For adsorbent dosage minimum removal percent, 62.7% was obtained at a minimum dosage (0.5g), and maximum removal percentage, 75.59% was obtained at higher adsorbent dosage (1g). This is because of the larger accessibility of active sites. In case of contact time against removal percentage reveals direct r/ship until equilibrium of removal percentage attains.From the one factor revealed below, minimum removal percentage, 62.11% was obtained at a contact time of 45min and maximum removal percentage, 76.21% was obtained at the contact time, 105min.

3.3.4. Interaction effects of initial Pb (II) concentrations and solution PH (AB)

Interaction effect of initial concentration and pH on removal efficiency of Pb (II) at the medium level (center point) of the contact time (75min), and adsorbent dosage (0.75g/100ml) was indicated in the figure 15. The percentage removal of Pb (II) ion increased with decreasing initial concentrations of Pb (II) and increased pH of the solution. As shown from the figure, the removal efficiency increases with increasing from pH, 3 to 6.5. It is known that the maximum removal percentage at all the initial concentrations takes place at pH 6.5. The maximum removal efficiency of very high was observed at constant adsorbent dosage (0.75g/100ml) and contact time (75min).

3.3.5. Interaction effects of initial lead (II) concentration and adsorbent dosage (AC)

The interaction effects of initial Pb (II) concentration and adsorbent dosage on the removal percentage were illustrated in figure 16. From the figure, it can be observed that the decrease in initial Pb (II) concentration and the increase in adsorbent dosage resulted in an increase in

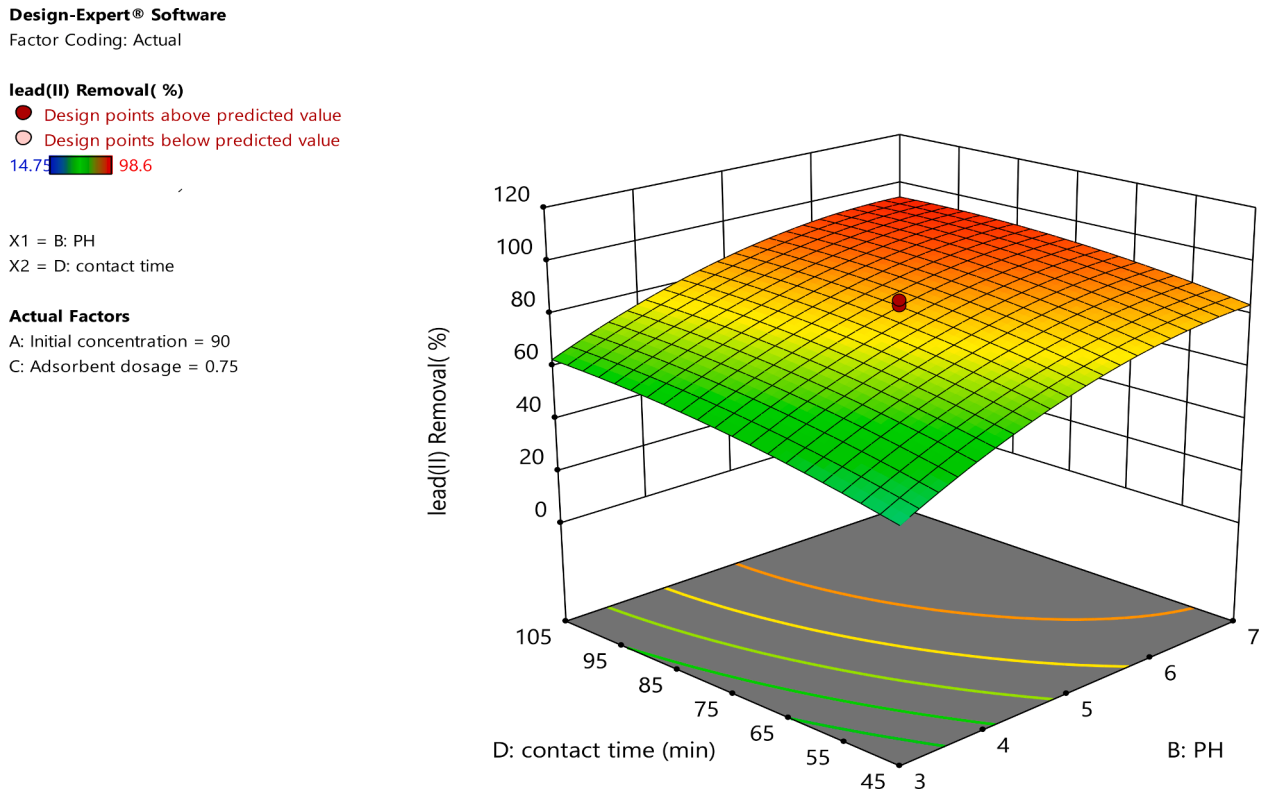

Fig. 19. Interaction effects of both pH and contact time on Pb (II) removal Response surface plot.

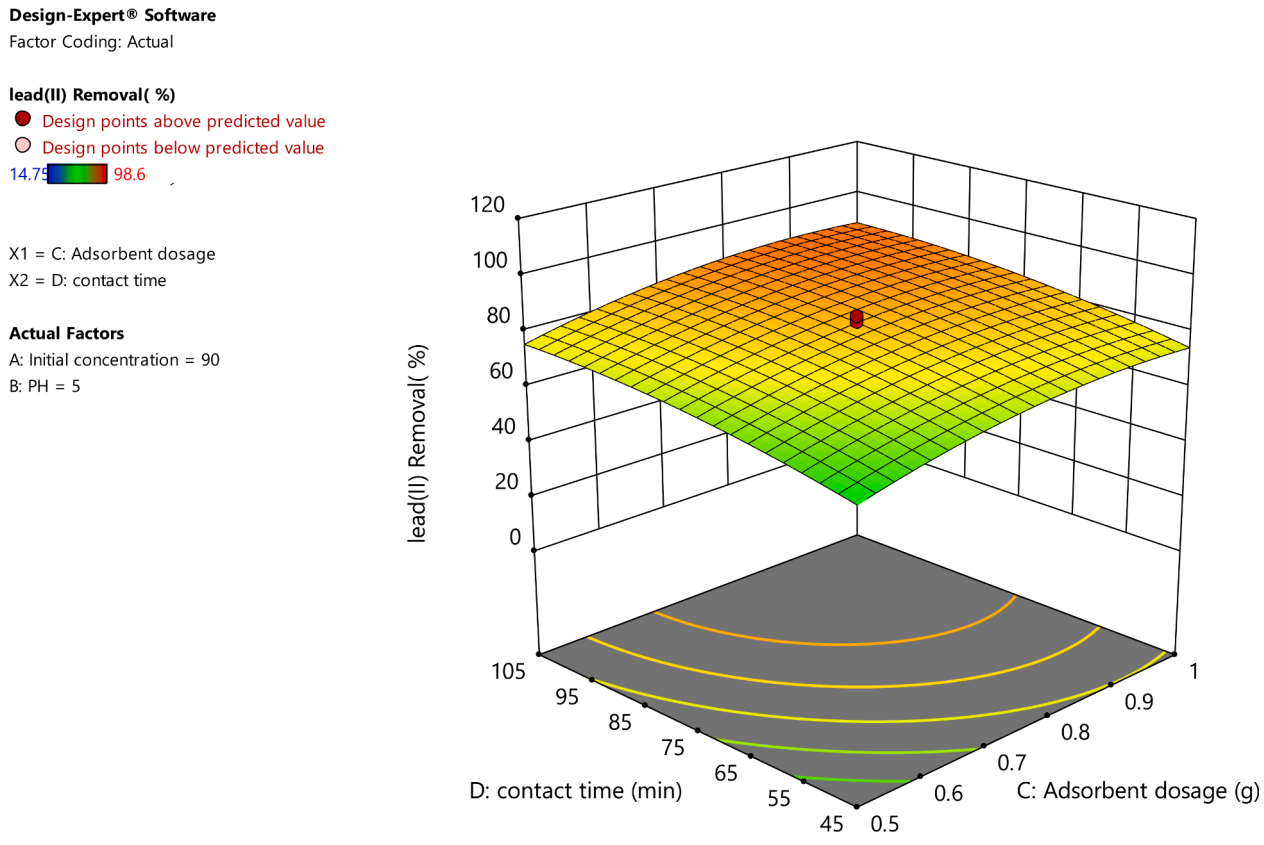

Fig. 20. Interaction effects of both adsorbent dosage and contact time on Pb (II) removal Response surface plot.

Table 8
Goals of the optimization and its ranges.

Variables	Ultimate goal	Experimental range Lower limit	Upper limit
Initial Pb (II) concentration (mg/L)	In the range	60	120
pH	In the range	3	7
Adsorbent dosage (g/100 ml)	In the range	0.5	1
Contact time (min)	In range	45	105
% removal of Pb (II)	Maximize	14.75	98.6

removal percent of Pb (II). The plot also showed that at higher PH value and the variation contact time has more effect on the percent removal of Pb (II) than the initial metal concentrations.

3.3.6. *Interaction effects of initial metal ion concentrations and contact time (AD)*

The combined effects of initial Pb (II) concentration and contact time on the percent removal of Pb (II) are indicated in figure 17. From the graph, the percent removal of Pb (II) increases as initial Pb (II) concentration decreases and contact time increases. A maximum removal percentage of Pb (II), 95.04% occurred at a contact time of 104min and an initial Pb (II) concentration of 61.5ppm.

3.3.7. *Interaction effects of PH and Adsorbent dosage (BC)*

Interaction effect of pH and dosage was illustrated in three dimensional and contour graph as indicated in figure 18 orderly. The percentage removal increases with increasing pH and dosage. At pH 6.96 and adsorbent dosage of 0.80813g, the lead (II) removal efficiency obtained was 92.9807%, when the remaining two variables (factors) place at the medium level (center point). The plot depicted that the removal of Pb (II) was extremely reliant on solution pH than adsorbent dosage. Generally, this demonstrates that the removal percentage was favorably more prominent by pH (Havva et al., 2014).

3.3.8. *Interaction Effect of PH and contact time (BD)*

The interaction effect of pH and contact time (BD) was depicted in three dimensional and contour chart as shown in figure 19. The efficiency of Pb (II) removal increases with increasing both solution pH and contact time. At pH 6.909 and contact time 115 min the Pb (II) removal efficiency obtained was 94.69% and the remaining two variables place at their medium level. As concluded from the plot the reduction of Pb (II) was extremely reliant on pH rather than contact time and the removal efficiency of Pb (II) was extremely prominent by pH. Generally as illustrated from the plot as contact time and pH increase the removal efficiency also increases and contrast declines as contact time and pH decrease.

3.3.9. *Interaction effect of adsorbent dosage and contact time (CD)*

As depicted from the figure below the combined effect of adsorbent dose and contact time for the removal of Pb (II). From figure 20, it can be observed that an increase in both contact time and adsorbent dosage resulted in increased removal efficiency of Pb (II). This is due to enough surface area available for adsorption (Sravan et al., D 2014).

3.3.10. *Optimization Parameters of lead (Pb (II)) removal by CaO NPs*

The optimization was conducted after interaction effects between adsorption parameters as shown in Table 8. Those optimum working

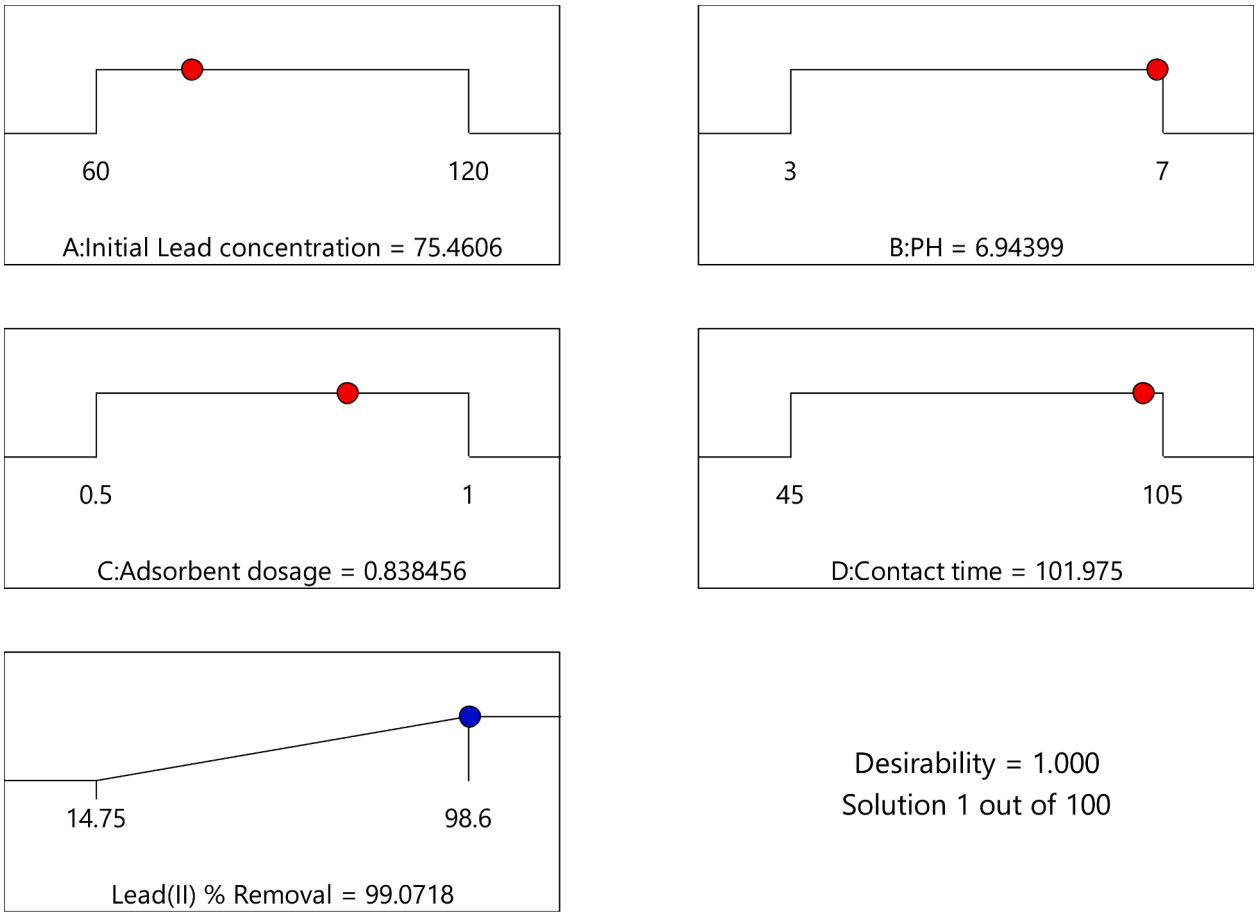

Fig. 21. Desirability ramp for numerical optimization for the selected variables using CaO NPs.

Table 9
Optimum conditions and model validation.

Variables	Optimum results
Initial Pb (II) concentrations (mg/L)	75.46
pH	6.94
Adsorbent dosage (g/100 ml)	0.838
Contact time (min)	101.97
% removal of Pb (II)	99.07
Experimental % removal of Pb (II)	98.86
Desirability	1

conditions of the possible goals of numerical optimizations were maximized, minimize, target, in range of the response (percentage removal of Pb (II)) and factors only (initial metals concentration, pH, adsorbent dosage, and contact time) which applied for the analysis of optimization. The targeted criterion was maximizing percentage removal of Pb (II) and were the other factors remained in a range. Design-Expert software version 11.1.2.0 was generated a set of solutions to determine the optimum conditions which had high composite desirability and removal efficiency. Desirability is the objective function. For any given response it ranges from zero to one. Value of one in desirability indicates the ideal case while zero represents one or more responses that fall outside the desirable limit. Optimizations of numerical show the point which would maximize the function of desirability.

The experimental percentage and predicted percentage values with percent removal of Pb (II) were explained below under validation experiments. A very small difference in percent between the experimental and predicted removal percentages of Pb (II) shows sufficient to predict the Pb (II) removal process using the adsorbent CaO NPs in the ranges of factors studied.

3.3.11. Validation Experiments

In order to verify the optimization results, an experiment was conducted under predicted conditions through the developed model. From figure 21, the model predicted 99.07% removal of Pb (II) at concentration 75.46mg/L, pH 6.94, adsorbent dosage 83.8g/L, and contact time 101.97min. Also, the experimental value obtained at these conditions of Pb (II) removal was 98.86% and was in close agreement with the result obtained from the model and hence validated the findings of the optimization. This experimental validation was the final step in the modeling process to investigate the accuracy of the established models. The results of predicted and experimental values of the output variables were indicated in Table 9. The maximum error (%) between the predicted and the experimental values was 0.21%, which is less than 3%, indicating that the quadratic models adopted could predict the experimental result well (Okolo et al., 2020). Hence, it can be concluded that the models accurately represent lead (II) ion removal over the experimental range studied. Dolatabadi et al., (2021a) also suggested that, Processing process optimization process has been executed Maximum using the developed model 99.1% DMP degradation achieved under optimal conditions 6 mA cm^{-2} current density, 4 mg L^{-1} initial DMP concentration, 600 µl $L^{-1}H_2O_2$ dose, electrolysis time of 8 minutes, solution pH of 3 and 50 mM Na_2SO_4 concentration. Trial results obtained The expected 99.6% efficiency was in good agreement.

4. CONCLUSIONS

Lead ion removal from aqueous solution using sol-gel derived calcium oxide nanoparticles, which was utilized as an effective and inexpensive sorbent for heavy metal removal particularly lead ions was investigated. The CaO NPs derived from low-cost waste hen eggshells become a better adsorbent The synthesized CaO particles from waste hen eggshell ensued an important increase in the specific surface area. Using central composite design, the optimum parameter conditions of 75.46mg/L initial Pb (II) concentration, 0.838g adsorbent dosage, pH 6.94 and contact time 101.07 min were determined to yield a maximum Pb (II) removal of 99.07%. This case was due to the fact that for a fixed adsorbent dosage, the overall available active sites were limited as a result leading to a decrease in removal percentage of the adsorbate, equivalently to an increase in initial adsorbate concentration. Langmuir isotherm model fitted very well to the data with correlation coefficients (R^2) of 0.9963. It indicates a monolayer formation over the surface of the material.The pseudo-first-order kinetic model fitted very well with the highest correlation coefficient (R^2) of 0.945. ANOVA results clearly imply that the models developed for adsorption of lead (II) ions onto CaO NPs were highly significant based on low P values. We conlude that the hen eggshell CaO NPs synthesized by the sol-gel process was superion lead removal sorbent can be utilized for the commercial treatment process.

Declaration of Competing Interest

The authors declare that they have no known competing financial interests or personal relationships that could have appeared to influence the work reported in this paper.

Supplementary materials

Supplementary material associated with this article can be found, in the online version, at https://doi.org/10.1016/j.sajce.2022.03.008.

References

Afroze, S., Sen, T., 2018. A review on heavy metal ions and dye adsorption from water by agricultural solid waste adsorbents. Water Air Soil Pollut. 225–229.

Safatian, Fatemeh, 2019. Lead ion removal from water by hydroxyapatite nanostructures synthesized from egg sells with microwave irradiation. Appl. Water Sci. 9–108.

Olesky, 1990. Removal and Recovery of Heavy Metals By Biosorption, 7. CRC Press, Boca Raton, FL.

EEPA. (1997). *Ethiopian Environmental Protection Authority. Annual Report.* Addis ababa, Ethiopia.

Stadelman, 2000. Eggs and egg products. In: Francis, F.J. (Ed.), Encyclopedia of Food Science and Technology, pp. 593–599.

Kaushal, Achla, Singh, SK, 2017. Adsorption phenomenon and its application in removal of lead from waste water: a review. Int. J. Hydrol. 1 (2), 38–47. :

Castro, J.C., 2011. Alternative low-cost adsorbent for water and wastewaterdecontamination derived from eggshell waste: an overview. Waste Biomass Valor 2, 157–167.

Adeyeye, 2009. Comparative study on the characteristics of eggshells of some bird species. Bull. Chem. Soc. Ethiopia 23, 159–166.

Fenta, M.M., 2014. Heavy metals concentrations in effluent of textile industry, tikur river and milk of cows watering on this water sources, hawassa, Southern Ethiopia. Reaearch J. Environ. Eng. 8 (8), 434, 422.

Fathia, 2017. Removal of lead and copper ion from polluted aqueous solutions using nano-saw dust particles. Int. J. Waste Resour. https://doi.org/10.4172/2252-5211.1000305.

Geeta, 2014. Tea wastes as sorbent for removal of heavy metals from wastewater. Int. current Eng. Technol. P-ISSIN 2347-5161.

Zhang, 2012a. Equilibrium, kinetics and thermodynamics studies of Lead (II) biosorption on Semame husks. BioResources 7 (3), 3555–3572.

Kumaraswamy, K., Dhananjaneyulu, B.V., Vijetha, P., Kumar, Y, 2015. "Kinetic and equilibrium studies for the removal of chromium using eggshell powder". Res. J. Pharmaceutical, Biol. Chem. Sci. 6 (1), 529–532.

Lulit Hapte, N.S., Mulatu, Dure, Thenepalli, Thriveni, Chilakala, Ramakrishna, Whan Ahn, Ji, 2019. Synthesis of nano-calcium oxide from waste eggshell by sol-gel method. Sustainability 11, 3196.

. Workeneh, Kifle, Z, E.A., Segne, Toshome Abdo, Eswaramoorthy, Rajalakshmanan, 2019. Eggshell-derived nanohydroxyapatite adsorbent for defluoridation of drinking water from bofo of Ethiopia J. Nanomater. 2019, 1–12. :

Balaganesh, A.S., R, S., Ranjithkumar, R., Chandarshekar, B., 2018. "Synthesis and characterization of porous calcium oxide nanoparticles (CaO NPS)". Int. J. Innovative Technol. Exploring Eng. (IJITEE) 2278–3075.

Ramachandran, Kasirajan, Sivakumar, Pandian, Suganya, Tamilarasan, Renganathan, Sahadevan, 2011. Production of biodiesel from mixed waste vegetable oil using an aluminium hydrogen sulphate as a heterogeneous acid catalyst. Bioresource Technol. 102, 7289–7293.

Li, Ye Li Zhenshan, Wang, Hui, Cai, Ningsheng, 2020. CaO carbonation kinetics determined using micro-fluidized bed thermogravimetric analysis. Fuel 264, 1–8.

Yadav, O.P., 2012. Adsorption of methylene blue on carbonized banana musa acuminata peel. Diss. Haramaya University.

Humaira, KHAN, M, J.A., BHANGER, M.Iqbal, 2007. "A rapid spectrophotometric method for the determination of trace level lead using 1, 5-diphenylthiocarbazone in aqueous micellar solutions". J. Analytical Sci. 23, 193–199.

Marandi, Reza, Sepehr, Seyedeh Marjan Bakhtiar, 2011. "Removal of orange 7 dye from wastewater used by natural adsorbent of *Moringa Oleifera* Seeds". Am. J. Environ. Eng. 1 (1), 1–9. https://doi.org/10.5923/j.ajee.20110101.01.

Huang, Yuan-dong, 2019. Comments on "Enhanced removal of Cr (Vl) from aqueous solution by supported ZnO nanoparticles on biochar derived from waste water hyacinth. Chemosphere 233, 993–994.

Bayuo, Jonas, P-B, K.B., Abukari, Moses Abdullai, 2019. "Optimization of adsorption parameters for effective removal of lead (II) from aqueous solution". Phys. Chem. An Indian J. : ISSN:0974 -7524.

BHAUMIK, R., N, K.M., DAS, B., ROY, P., PAL, K.C., DAS, C., BANRJEE, A., DATTA, J.K., 2012a. "Eggshell powder as an adsorbent for removal flouride from an aqueous solution.Equilibrium, kinetics and thermodynamic studies". E- J. Chem. 1457–1480.

Getasew Ketsela, Z.A., Talema, Alemu, 2020b. "Adsorption of Lead (II), Cobalt (II) and Iron (II) From aqueous solution by activated carbon prepared from white lupine (GIBITO) HSUK". J. Thermodynamics and Catalysis 2157–7544.

Ajala, E.O., Eletta, O.A.A., Ajala, M.A., Oyeniyi, S.K., 2018. Characterization And Evaluation Of Chicken Eggshell For Use As A Bio-Resource, 14. Arid Zone Journal of Engineering, Technology and Environment, pp. 26–40. March, 2018.

Aljeboree, Aseel M., Alshirifi, Abbas N., Alkaim, Ayad F., 2017. Kinetics and equilibrium study for the adsorption of textile dyes on coconut shell activated carbon. Ar. J. Chem. 10 (2), S3381–S3393.

Zahra marghiasi, F.B., Darezereshki, Esmaeel, Esmaelizadeh, Esmat, 2014. "Preparation and characterization of CaO nanoparticles from calcium hydroxide by direct thermal decomposition method". J. Ind. Eng. Chem. 113-11.

Blazquez, G., M, A.M.-L., Tenorio, G., Calero, M., 2010. "Batch biosorption of lead (II) from aqueous solutions by olive tree pruning waste:Equilibrium, kinetics and thermodynamic study". Chem. Eng. J. 170–177.

Zaman, T., M, S.M., Mahmood, Md.A.Al, Rahman1, S., 2018. "Evolution and characterization of eggshell as a potential candidate of raw material". Ceramica 64, 236–241.

BHAUMIK, R., N, K.M., DAS, B., ROY, P., PAL, K.C., DAS, C., BANRJEE, A., DATTA, J.K., 2012b. "Eggshell powder as an adsorbent for removal flouride from an aqueous solution.Equilibrium, kinetics and thermodynamic studies". E- J. Chem. 1457–1480.

Viriya-empikul, N., Krasae, P., Nualpaeng, W., Yoosuk, B., Fau-ngnawakij, K., 2012. Biodiesel production over Ca-based solid catalysts derived from industrial wastes. Fuel 92, 239–244.

Gupta, VK, 2004. Removal of Pb (II) and Chromium from waste water using bagasse fly ash-a sugar industry waste. J. Colloid Interface Sci 271 (2), 321–328.

Moo-Yeal, Lee, S-H, L., Hyun-Jae, Shin, Toshio, Kajiuchi, Ji-Won, Yang, 2017. Characteristics of lead removal by crab shell particles. Process Biochem. 33, 749–753.

Yusuff, Adeyinka Sikiru, Olateju, Idowu Iyabo, Ekanem, Sophia Emmanuel, 2017. Equilibrium, kinetic and thermodynamic studies of the adsorption of heavy metals from aqueous solution by thermally treated quail eggshell. J. Environ. Sci. Technol. 10, 245–257.

Farghali, A.A., M, B., Enaiet Allah, A., Khedr, M.H., 2013. "Adsorption of Pb (II) ions from aqueous solutions using copper oxide nanostructures". J. Basic and Appl. Sci. 61–71.

Okolo, B.I., E, O.O., Agu, Chinedu M., Adeyi, O., Nwoso-Obieogu, K., Akatobi, K.N., 2020. Adsorption of lead (II) from aqueous solution using Africa elemi seed, mucuna shell and oyster shell as adsorbents and optimization using Box–Behnken design". Appl. Water Sci. 10, 201.

Havva, T, T, S., Yigitarslan, Y, 2014. "Optimization of lead adsorption of mordenite by response surface methodology: characterization and modification". J. Environ. Health Sci. Eng. 12, 11–19.

Sravan Kumar, D, R, V., Dayana, K, Sowjanya, CVN, 2014. "Application of response surface methodology (RSM) for the removal of nickel using rice husk ash as biosorbent". Int. J. Eng. Res. Gen. Sci. 2, 162–176.

Das, Payel, Nisa, Saimatun, Debnath, Animesh, Saha, Biswajit, 2020a. "Enhanced adsorptive removal of toxic anionic dye by novel magnetic polymeric nanocomposite: optimization of process parameters". J. Dispersion Sci. Technol. https://doi.org/10.1080/01932691.2020.1845958.

Bhowmik, Mahashweta, Debnath, Animesh, Saha, Biswajit, 2019a. Fabrication of mixed phase CaFe2O4 and MnFe2O4 magnetic nanocomposite for enhanced and rapid adsorption of methyl orange dye: statistical modeling by neural network and response surface methodology. J. Dispersion Sci. Technol. https://doi.org/10.1080/01932691.2019.1642209.

Das, P, Debnath, A, Saha, B, 2020b. Ultrasound-assisted enhanced and rapid uptake of anionic dyes from the binary system onto MnFe2O4/polyaniline nanocomposite at neutral pH. Appl. Organomet Chem.: 5711. https://doi.org/10.1002/aoc.5711.

Deb, A, Debnath, A, Saha, B, 2019. "Ultrasound-aided rapid and enhanced adsorption of anionic dyes from binary dye matrix onto novel hematite/polyaniline nanocomposite: Response surface methodology optimization". Appl. Organometal Chem. e5353 https://doi.org/10.1002/aoc.5353 https://doi.org/.

Deb, Akash, Debnath, Animesh, Bhattacharjee, Nilanjana, Saha, Biswajit, 2020. "Ultrasonically enhanced dye removal using conducting polymer functionalised ZnO nanocomposite at near neutral pH: kinetic study, isotherm modelling and adsorbent cost analysis". Int. J. Environ. Analytical Chem. https://doi.org/10.1080/03067319.2020.1843649.

Dolatabadi, Maryam, Swiergosz, Tomasz, Ahmadzadeh, Saeid, 2021a. "Electro-Fenton approach in oxidative degradation of dimethyl phthalate - The treatment of aqueous leachate from landfills". Sci. Total Environ. 772, 145323.

Dolatabadi, Maryam, Taghi Ghaneian, Mohammad, Wang, Chongqing, Ahmadzadeh, Saeid, 2021b. Electro-Fenton approach for highly efficient degradation of the herbicide 2, 4-dichlorophenoxyacetic acid from agricultural wastewater: Process optimization, kinetic and mechanism. J. Mol. Liquids 334, 116116.

Ahmadzadeh, Saeid, Rezayi, Majid, Karimi-Maleh, Hassan, Alias, Yatimah, 2015. Conductometric measurements of complexation study between 4-Isopropylcalix[4] arene and Cr3+ cation in THF–DMSO binary solvents. Measurement 70, 214–224.

Fouladgar, Masoud, Ahmadzadeh, Saeid, 2016. Application of a nanostructured sensor based on NiO nanoparticles modified carbon paste electrode for determination of methyldopa in the presence of folic acid. Appl. Surface Sci. 379, 150–155. https://doi.org/10.1016/j.apsusc.2016.04.026.

Rezayi, M., et al., 2014. Titanium (III) cation selective electrode based on synthesized tris (2pyridyl) methylamine ionophore and its application in water samples. Sci. Rep. 4, 4664. DOI:10.1038/srep04664 (2014).

Rounaghi, G.H., Mohajeri, M., Ahmadzadeh, S., Tarahomi, S., 2009. A thermodynamic study of interaction of Na+ cation with benzo-15-crown-5 in binary mixed non-aqueous solvents. J. Incl. Phenom. Macrocycl. Chem. 63, 365–372. https://doi.org/10.1007/s10847-009-9530-0.